Environmental Science Nano

ROYAL SOCIETY OF CHEMISTRY

PAPER

Cite this: DOI: 10.1039/d4en01077a

Catalytic performance of electronic waste-derived gold nanoparticles for the reduction of *p*-nitrophenol†

Michelle Y. Lau, *[a] David C. Young, [b] Jack L.-Y. Chen [cde] and Jonathan Sperry *[a]

Received 18th November 2024,
Accepted 30th December 2024

DOI: 10.1039/d4en01077a

rsc.li/es-nano

Current methods for producing gold nanoparticles (AuNPs) typically involve solutions containing 50 to 27 000 ppm of gold. These precursor solutions are derived from purified ore material and are not representative of waste-derived gold-containing solutions, which generally range from 20 to 30 ppm. Electronic waste (e-waste) is an increasing global concern due to the presence of various toxic substances that can leach into the environment and pose risks to human health. However, e-waste also represents a rich source of precious metals, including Ag, Pd, and Au. Here, we report the synthesis of AuNPs derived from $AuCl_4^-$ or AuI_4^- at concentrations typical of e-waste streams, as well as from printed circuit board (PCB) e-waste samples. The AuNPs, ranging from 3 to 30 nm in diameter, are deposited onto commercially available cellulose fibres by a reductive deposition method using hydrazine hydrate. The catalytic performance of the AuNPs was evaluated in the reduction of *p*-nitrophenol to *p*-aminophenol in the presence of $NaBH_4$. The AuNPs derived from e-waste on cellulose exhibited higher turnover number (TON) and turnover frequency (TOF) compared to commercially available 30 nm AuNPs and previously reported AuNPs on cellulose, possibly due to trace amounts of palladium present. This study demonstrates that AuNPs can be efficiently synthesised from e-waste streams and provides proof-of-concept evidence that the gold in bulk e-waste can serve as a valuable source of high-value catalysts.

Environmental significance

Gold nanoparticles (AuNPs) have a wide range of applications in biomedicine, sensing, and catalysis. AuNPs are typically synthesised from gold salts derived from gold ore, in which the mining of these materials imposes a significant environmental and socioeconomic burden. In this study, we demonstrate that catalytically active AuNPs can be produced using gold recovered from bulk electronic waste, specifically printed circuit boards (PCBs). Herein, we report and highlight several new aspects of e-waste-derived AuNPs and how they affect catalytic performance, including trace palladium content. The derived AuNPs are also from a bulk source of e-waste, not chips or gold chips off PCBs, which initially have a high gold concentration. Additionally, our AuNPs derived from electronic waste exhibited superior catalytic properties to an analogous material created from highly refined materials in the reduction of *p*-nitrophenol, providing proof-of-concept evidence that the gold in bulk e-waste can serve as a valuable source of high-value catalysts. Through utilisation of a waste product, the biopolymer cellulose and the green oxidant TCCA, we have demonstrated the production of a high-value catalyst that shows superior performance to equivalents derived from stock gold solutions.

Introduction

Gold has traditionally been regarded as one of the least reactive metals.[1] However, its reactivity changes dramatically at the nanoscale, particularly in the form of gold nanoparticles (AuNPs), which possess unique physical and chemical properties that have been investigated for applications ranging from nanomedicine[2] (such as biolabeling, diagnostics and drug delivery) to catalysis.[3]

Interest in AuNPs has increased significantly over the last few decades due to their unique characteristics as nanomaterials. Michael Faraday first documented an aqueous solution of colloidal gold nanoparticles in the 1850s, and he is widely credited for the "first" scientific discussion on size-dependent optical properties and their coagulation behaviour.[4] A century later, Turkevich *et al.*, using electron microscopy, confirmed that Faraday's ruby-coloured colloidal solutions had an average size of 6 ± 2 nm.[5]

[a] *Centre for Green Chemical Science, University of Auckland, Auckland, New Zealand. E-mail: mlau527@aucklanduni.ac.nz, j.sperry@auckland.ac.nz*
[b] *Mint Innovation, 6 Hotunui Drive, Auckland, New Zealand*
[c] *School of Science, Auckland University of Technology, New Zealand*
[d] *The MacDiarmid Institute, Victoria University of Wellington, PO Box 600, Wellington 6140, New Zealand*
[e] *Department of Biotechnology, Chemistry and Pharmaceutical Sciences, Universitá degli Studi di Siena, Italy*

† Electronic supplementary information (ESI) available. See DOI: **https://doi.org/10.1039/d4en01077a**

In the 1980s, Hutchings and Haruta's groundbreaking findings revealed the catalytic capabilities of gold and laid the foundations for gold salt and nanoparticulate catalysis. In 1991, it was reported that cationic gold supported on carbon could catalyse the hydrochlorination of acetylene to vinyl chloride.[6] Haruta and coworkers used coprecipitation of metal nitrates and chloroauric acid with sodium carbonate, followed by calcination, to prepare metal oxide (MO)-supported AuNP catalysts for CO oxidation.[7] These seminal findings sparked extensive interest in the catalytic applications of AuNPs and gold salts. Currently, gold(0) nanoparticles have found applications in numerous organic transformations, including hydrogenations,[8–10] nitro group reductions,[11,12] activation of alkynes,[13–23] oxidation of alcohols,[24–32] and coupling[33–42] reactions.

AuNPs can be prepared using chemical, sonochemical, or photochemical methods.[43] The most commonly used methods are chemical processes, which typically involve the precipitation of a dissolved gold salt in an aqueous medium, usually in the form of chloroauric acid or an alkali tetrachloroaurate.[44–52] The widespread use of these gold chlorides is due to the relative ease and speed of oxidative gold dissolution in chloride-containing media.

Various green procedures for AuNP synthesis have been reported, with the majority utilising plants high in metabolites such as terpenoids, polyphenols, alkaloids, and phenolic acid to bio-reduce the gold ions into their nanoparticulate forms.[53] Coconut oil,[54] orange,[55–57] pomegranate, banana,[58,59] watermelon,[60] and avocado peels[61] have all been reported to bio-reduce and synthesise AuNPs. Electrochemical extraction has also been reported,[62] as well as laser ablation techniques using palm oil.[63] In all these cases, the gold solution used for AuNP formation is derived from commodity-grade gold that has been subjected to a refining process that is both energy intensive and expensive. While a great deal of work has been conducted with the aim of decreasing the environmental impact of the reductant or support material used in the formation of AuNPs, the origin of the gold precursor is often ignored. With growing interest in urban mining and its role in enabling a circular economy, increased attention should be paid to waste stream-derived materials as the source of the gold required for AuNP synthesis (Scheme 1).

Various works have been reported the recovery of Au^{3+} ions using polymeric films, hydrogels and as complexes derived from e-waste.[64,65] Recovery of Pt^{2+} from catalytic convertors has also been reported using hydrogels.[66] Park reported the synthesis of gold nanoparticles (AuNPs) derived from printed circuit boards (PCBs) using toluene extractions of the PCB leachate solution.[67] Phospholipids, combined with an AC voltage of 100 V, have also been utilised to recycle metallic waste-derived gold into AuNPs. These nanoparticles were then collected by centrifugation, resulting in a solid containing less than 6 wt% gold.[68] The use of biomass, such as cyanide-producing bacteria, to leach gold from waste and synthesise AuNPs has also been reported.[69] AuNPs from waste-derived

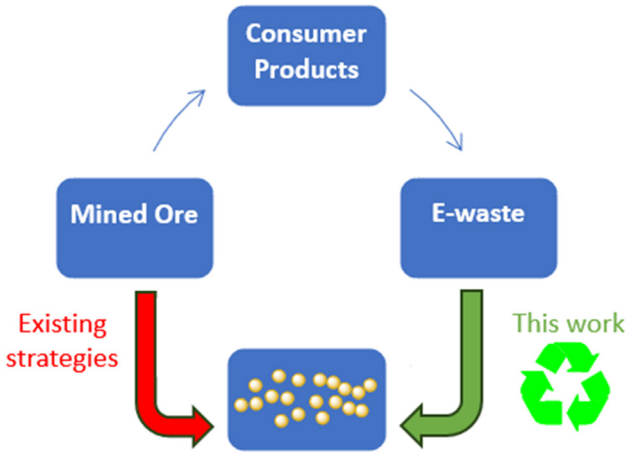

Scheme 1 Methods for AuNP production from mined gold ore far outweigh those that use waste-derived materials.

materials using red raspberry leaf extracts high in catecholamine-containing anthocyanins to bioreduce Au^{3+} have also been reported.[70] Catecholamine groups preferentially coordinate with gold ions (Au^{3+}) to form complexes, that may lead to initiation of nucleation for seed formation.[71]

Despite the growing number of studies on the formation of AuNPs from waste materials, few investigations have yet been conducted on the applications of the nanomaterials produced. AuNPs derived from waste have been shown to be active in the catalytic oxidation of CO and methanol and the reduction of *p*-nitrophenol.[72–75] However, the methods utilised required a manual physical process of removal of CPU boards, gold pins and even gold flakes off PCBs, or pre-purification of Au, which is not representative of realistic large-scale recycling methods. The initial starting concentration for the reported methods ranged from 180–200 ppm, approximately 9 to 10 fold higher than a hydrometallurgical leach of whole PCBs.[72–75] The reported reduction of *p*-nitrophenol was also reported to have utilised a significant excess of $NaBH_4$ (500 mol eq.) and Au (1800 mol%).[75] Au^{3+} complexes recovered from e-waste that were catalysts for the cyclisation of propargylic amides and condensation of acetylacetone with *o*-iodoaniline have been reported.[76] However, the methods utilised are again not representative of large-scale recycling methods, as high temperature (reflux) and solvents such as THF, HCl, and vapour deposition methods were utilised.

In this study, we report the production, characterisation, and optimisation of AuNPs derived from end-of-life circuit boards and demonstrate their catalytic activity through the reduction of *p*-nitrophenol which is commonly used as a model system.[44,46,48–52,77,78] Differences in catalytic activity between AuNPs derived from stock solutions and AuNPs derived from e-waste were found and investigated further.

Electronic waste

A wide range of products are classified as electrical and electronic equipment (EEE), including large and small

household appliances, as well as information and communication technology devices such as computers, cellular phones, telecommunication equipment, and portable electronics. Once these products reach the end of their useful life, they become electronic waste (e-waste). Rapid urbanisation, advancements in science and technology, increased consumer usage, and a throw-away culture have made e-waste an exponentially growing problem worldwide. The amount of e-waste generated globally increased by 21% in five years from 2014 to 2019.[79] In 1994, an estimated 20 million personal computers (PCs) became obsolete, accounting for 7 million tonnes of waste alone.[80] In 2004, the number of obsolete PCs increased to 100 million.[80] In the US alone, 500 million computers became obsolete between 1997 and 2010, while in Japan, 610 million computers were discarded by the end of 2010.[79] Globally, e-waste accounted for 8% of waste in 2005 to become the fastest-growing waste stream and accounted for 53.6 million metric tonnes of waste in 2019.[79,81]

Printed circuit boards (PCBs) are an integral part of all electrical and electronic equipment (EEEs), as they provide both electrical connections and mechanical support for the electronic components.[82] The exact components of PCBs depend highly on the final function of the EEEs, but they usually comprise ~30–40% metals, ~30% plastics, and ~30% ceramic materials.[83] Annually, over US$80 billion of valuable metals are discarded in consumer and industrial waste streams, which provides a source of urban-derived anthropogenic material that can be reused, giving rise to the term "urban mining".[84,85] The major metallic components are comprised of Cu (20–30 wt%), Fe (4 wt%), Al (3.3 wt%), and Sn (2.6 wt%). Urban mining is rapidly emerging as a viable alternative to traditional mining, which often results in irreversible environmental and socioeconomic consequences. The metal content in relevant ores is significantly lower than in PCBs.[86] Copper ore contains 0.5–1% copper and currently mined gold ore usually ranges from 1–10 g T^{-1}, both being approximately 20 × lower than in PCBs.[86,87]

The two primary methods for recovering gold and other precious metals from e-waste are pyrometallurgy and hydrometallurgy.[87] Pyrometallurgical processing is the most traditional and widely used industrial method for recovering gold and other precious metals.[87] It involves incinerating and smelting in a plasma arc at high temperatures, using base metal absorbers (Cu and/or Pb) in the presence of slag to concentrate the precious metals and remove plastic and carbon impurities.[87] The resulting Au, Ag, and platinum group metal (PGM) alloy is further refined through hydrometallurgical processes, which include leaching, solvent extraction, and subsequent precipitation or electrodeposition.[87] Standard hydrometallurgical processes include halide leaching (chlorine, bromine and iodine), thiourea, thiosulfate, and the industrial standard cyanide leaching methods.[83,88] Due to the detrimental effects and carbon emissions associated with pyrometallurgical processes, we chose to use non-pyrolysis-pretreated e-waste and focus our efforts on the hydrometallurgical digestion of raw e-waste.

The primary objective of this study was to investigate whether gold recovered from e-waste could serve as a sustainable precursor for catalytically active AuNPs. The utilisation of e-waste provides a greener alternative to mining virgin material, especially in the case of gold due to the approximately 40 times lower concentration in currently mined ores compared to PCBs. Reduced land and water usage in addition to avoidance of toxic cyanide reagents also provides green benefits. Initial experiments were conducted with gold solutions at concentrations simulating those found in the leachate from non-pyrolysed e-waste, which can realistically reach 20–30 ppm of gold after hydrometallurgical leaching. After optimising this model system, the synthetic process was applied to PCB e-waste, and the catalytic activity of the resulting AuNPs was compared to that of commercially available AuNPs.

Experimental section

Chemicals and reagents

Fine gold, palladium, and silver were purchased from Regal Ltd. Ascorbic acid was sourced from Davis Food Chemicals. Squaric acid, *p*-nitrophenol, chitosan, gold nanoparticles (30 nm, citrate stabilised) were sourced from Sigma-Aldrich. Hydrazine hydrate (80%), trisodium citrate, starch, sodium hydroxide AR pearls, hydrochloric acid (33%), and nitric acid (69%) were sourced from ECP Ltd. Cellulose fibres were obtained from E. Begerow GmbH. Chitin and $NaBH_4$ were sourced from AK Scientific. All glassware was washed with *aqua regia*, rinsed with de-ionised water and oven-dried prior to use.

Preparation of AuNPs

Fine gold was digested with *aqua regia* ($HCl:HNO_3$ 4 : 1)[89,90] or an iodide leach[91–94] to create 1000 ppm stock solutions. 20 ppm $AuCl_4^-$ and AuI_4^- solutions were prepared from 1000 ppm stock solutions by dilution with 3% HCl or KI solutions. The support material (10–14 g L^{-1}) was added before the addition of the corresponding reductant (300–620 molar equivalents). The AuNPs loaded on the support were washed with 3% HCl or KI and dried in the oven overnight at 60 °C. Printed circuit boards were obtained from Mint Innovation Ltd (NZ), and subjected to a base metal leach using H_2SO_4 and H_2O_2 prior to use.[95–99] Three 20 g samples of base-metal leached e-waste were subjected to a thermal *aqua regia* digest at 60 °C for 3.5 h to determine the residual base-metal and gold content (Table S4, ESI†). The residual metals, including gold, were leached using TCCA.[100–105] Briefly, e-waste was slurried in a 42 g L^{-1} TCCA solution and heated at 40 °C for 4 hours, followed by filtration. Residual chlorine was decomposed by adding H_2O_2. The gold concentration in the solution was measured using AAS, and AuNPs were subsequently deposited onto

the support using the optimal reductant to produce the PCB e-waste sample.

AAS and MP-AES

After dissolving the catalyst into *aqua regia* ($HCl:HNO_3$ 4 : 1), the gold content of the model system catalyst and PCB e-waste sample was determined using a Shimadzu atomic absorption spectrophotometer 6300 using a gold lamp (λ = 242.8 nm, slit = 0.7 nm). The palladium content was obtained using atomic absorption spectroscopy (AAS) with a palladium lamp (λ = 246.6 nm, slit = 0.7 nm). The base-metal content of the PCB e-waste sample was determined using an Agilent 4200 MP-AES after an *aqua regia* digest.

XPS

A Kratos Axis DLD XPS system was used to investigate the chemical properties and changes in binding energies of the model systems and e-waste-derived samples. The system utilised monochromatic aluminum Kα X-rays (1486.69 eV) with an X-ray source operating at 150 W. A charge neutraliser was employed to counteract potential surface charge buildup. Samples were mounted using double-sided adhesive tape. Data processing was performed using Casa XPS, with the C 1s signal from saturated hydrocarbons (285 eV) serving as an internal standard to correct the binding energy scales.

UV-vis

Absorbance spectra were recorded on Horiba Scientific Duetta fluorescence and absorbance spectrometer or Agilent Cary 60 UV-vis spectrometer.

DLS

DLS and zeta potential analysis were performed with a ZetaSizer Nano ZS (Malvern Instruments); data analysis was supported by Zetasizer v.2.2. DLS experiments were performed using disposable polystyrene cuvettes (DTS0012) or disposable folded capillary cells (DTS1070), with an assumed water viscosity of 25 °C (η = 0.8872 mPa).

TEM

Standard TEM images were recorded on an FEI Tecnai 12 with Gatan cold stages and a Gatan Ultrascan 100 4 Mpixel digital camera. Image processing was performed using ImageJ.JS.

SEM

Standard SEM images were recorded using a Hitachi SU-70 Schottky field emission scanning electron microscope. The specimens were sputter-coated with platinum (Pt) or carbon (C) for 60 seconds using a Hitachi E-1045 ion sputter. The composition of the particles was analysed by energy dispersive X-ray spectrometry (EDS) with a Noran System 7 (NSS) microanalysis system. Image processing was performed using ImageJ.JS.

Kiln

A muffle furnace with a high-temperature ceramic element kiln with a maximum temperature of 1750 °C was utilised. Bone ash cupels and ceramic crucibles were used for fire assay purposes.

Preparation of solid supports

Cellulose, chitin, chitosan, lecithin and starch were used as received. Micronised cellulose was synthesised as previously reported by Huang.[106] The polysulfide and carbonised polysulfide materials were synthesised as previously reported by Chalker and co-workers.[107,108] Carbonised cellulose was synthesised following an identical carbonisation procedure used for the carbonised polysulfide material.

Catalytic reduction of *p*-nitrophenol

A stock solution was prepared using *p*-nitrophenol (90 mg, 0.65 μmol) and $NaBH_4$ (180 mg, 4.78 μmol) in deionised water (50 mL). 2 mL of the stock solution was added to a suspension of AuNPs on cellulose in water (4 mL). The reaction mixture was sampled at fixed intervals and filtered through a 0.45 μm membrane filter. The absorption spectra of the filtrate were measured in the range of 250–500 nm. Kinetic rate constants were determined by applying a logarithmic function to the change in absorbance at 400 nm, correlating to the *p*-nitrophenolate ion over time. Compounds were also purified by flash column chromatography on silica gel and analysed by comparison with ^1H and ^{13}C NMR spectroscopic data. NMR spectra were recorded at room temperature in $CDCl_3$ solution using a Bruker DRX400 spectrometer operating at 400 MHz for ^1H nuclei and 100 MHz for ^{13}C nuclei. Chemical shifts are reported in parts per million (ppm) from tetramethylsilane (δ = 0) and were measured relative to the deuterated solvent in which the sample was analysed.

Results and discussion

To the best of our knowledge, the development of a functional heterogeneous AuNP catalyst using gold salt concentrations representative of e-waste has not been reported. Current literature procedures for generating catalytically active AuNPs typically use gold concentrations ranging from 50 to 27 000 ppm, which does not reflect the low gold concentrations found in e-waste leachate, typically ranging from 10 to 30 ppm.[44,46,48,50–52,109] Waste-derived supports have been reported, but the source of the noble metals for nanoparticulate materials is largely ignored.[110,111] Often, the remaining gold-containing lixiviants are also discarded, resulting in downstream waste-water implications. As an example, Camilo and collaborators synthesised a AuNPs loaded onto cellulose films using a starting gold concentration of 179 ppm, but after deposition, a residual 45 ppm remained in solution, making this cost prohibitive from an industrial perspective.[52]

In this study, we report the optimisation of AuNP synthesis from gold concentrations representative of waste streams and explore their potential application as catalysts. Due to the initially low gold concentrations in waste streams, the optimisation prioritised achieving high loading efficiencies onto supports to minimise wastewater generation.

External reductants are needed to convert gold salt precursors, typically $AuCl_4^-$ or AuI_4^-, into their nanoparticulate form and onto a support material to create a heterogeneous catalyst. Colloidal nanoparticulate solutions, though not requiring a heterogeneous support, follow a similar reduction pathway in the presence of capping agents to form AuNPs from gold salt precursors, as shown in Scheme 2. In this study, we investigated various support materials, reductants, and temperatures to assess their impact on the catalytic function of the synthesised AuNPs, evaluated by their ability to reduce *p*-nitrophenol to *p*-aminophenol.

Reductant screen

Initial experiments investigated the effectiveness of a series of reductants, namely ascorbic acid, trisodium citrate, sodium borohydride, and hydrazine hydrate, to form AuNPs from gold solutions representative of PCB leachate. The $AuCl_4^-$ model system was chosen due to the oxidative chloride leach being the most commonly used leachate for e-waste.[89,112–114] Other halide leaching methods for gold include iodide- and bromide-based systems, with iodide being more widely reported.[92,94,115,116] As such, AuI_4^- was chosen as a second model system which, to the best of our knowledge, has not been previously reported for the formation of AuNPs. Non-stable gold leachates using reagents such as thiourea and thiosulfate were not pursued. Cyanide-based model systems were not pursued due to their associated toxicity.

E-waste loadings for gold leaching have been reported to be between 1–50%, but on average usually range from 20–30%.[115,117–119] PCBs, on average, are 0.01 wt% Au, and assuming 20% solid loading in the leaching solution, a 20 ppm gold solution would be achieved.[87] Hence, 20 ppm stock solutions for both the $AuCl_4^-$ and AuI_4^- model systems were made, emulating typical PCB leachate solutions.

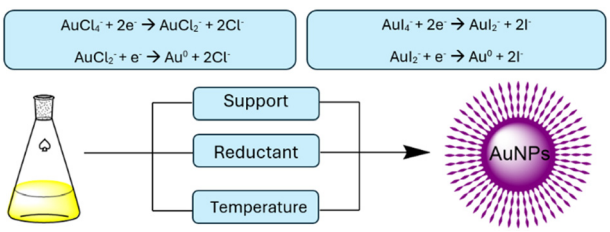

Scheme 2 Variables investigated (support, reductant, and temperature) for generating AuNPs from $AuCl_4^-$ and AuI_4^- precursor salts.

The AuNPs were generated by adding either ascorbic acid (300 eq.), trisodium citrate (300 eq.), sodium borohydride (300 eq.), or hydrazine hydrate (300 eq.) to 20 ppm solutions of either $AuCl_4^-$ and AuI_4^-. DLS measurements showed that the hydrodynamic size of the generated AuNPs was the smallest for hydrazine hydrate (1–50 nm for $AuCl_4^-$, 100–500 nm for AuI_4^-), intermediate for $NaBH_4$ (100–1000 nm), and largest for ascorbic acid and trisodium citrate (Fig. 1). Both ascorbic acid and trisodium citrate produced particles that were significantly larger than 1 μm and out of the detection range of the instrument. These trends were observed for both the $AuCl_4^-$ and AuI_4^- model systems, making hydrazine hydrate the most effective reductant to produce AuNPs with a small hydrodynamic radius. However, an increase in the hydrodynamic diameter was observed over time, indicative of continuous growth in the size of the AuNPs for the studied reductants. This phenomenon was observed with all samples, with the effect being more pronounced for the AuI_4^- samples compared to $AuCl_4^-$, except for $NaBH_4$ which appeared to be relatively stable. Measurement of the zeta potential for each of the samples was also attempted, but a stable reading could not be obtained, further suggesting poor colloidal stability in these samples and emphasising the need for a stabilising agent or a solid support.

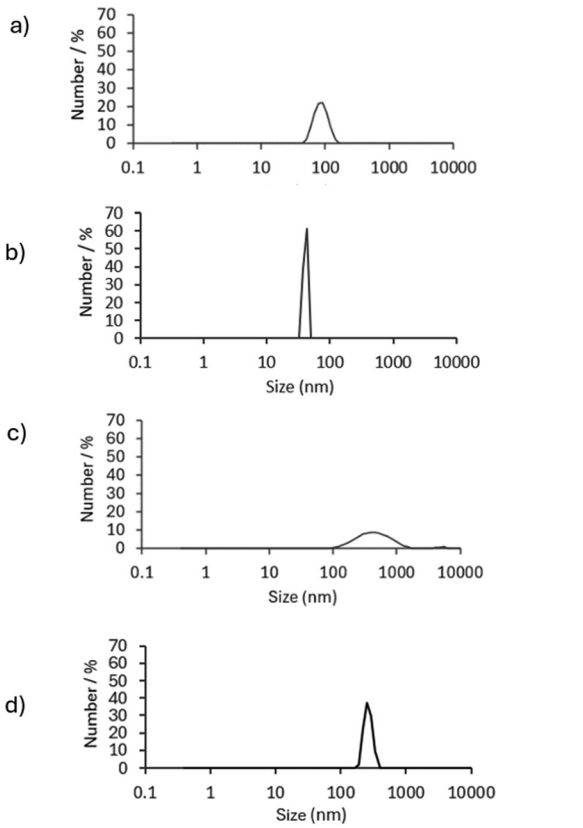

Fig. 1 DLS measurements of a) $NaBH_4$ in $AuCl_4^-$ model system, b) free-base hydrazine in $AuCl_4^-$ model system, c) $NaBH_4$ in AuI_4^- model system, d) free-base hydrazine in AuI_4^- model system.

Trisodium citrate was investigated for its ability to stabilise the AuNPs formed from free-base hydrazine. When sodium citrate was added at room temperature together with hydrazine for the $AuCl_4^-$ model system, the observed hydrodynamic size was 10 to 500 nm (Fig. S1, ESI†). However, the widely used Turkevich method involves addition of trisodium citrate to the gold salt precursor solution at reflux.[5,120] Our attempts at AuNP formation at higher temperatures resulted in the formation of much larger AuNPs. For example, AuNP formation at 70 °C, with a combination of trisodium citrate and free-base hydrazine does have a stabilisation effect on the size of the AuNPs, but forms much larger particles with a diameter of ~500 nm (Fig. S2, ESI†).

Effect of solid supports

Following the observations of instability in the AuNP colloidal solutions, various solid supports were investigated in attempts to stabilise the generated AuNPs. Anchoring metal nanoparticles onto metal oxide, carbon-based, zeolite and polymer supports is a widely used method to stabilise AuNPs for catalysis.[121] Cellulose, being the most abundant biopolymer on earth, has widely been reported as a support for AuNPs, and was of primary interest in our studies.[122] Chitin is the second most abundant biopolymer and has been reported as a suitable AuNP support, and was also investigated.[123,124] Alternatively, polysulfide materials were investigated due to its ability to be produced from elemental sulfur, an abundant industrial waste product.

Polysulfide materials have gained traction in environmental remediation for the removal of metals such as Fe(III), Cr(III), Co(II), Ni(II), Cu(II), Al(III), Ga(III), Ag(I), Cd(II), In(III), Ba(II), Hg(II), Pb(II), and Bi(III) from wastewater streams.[107,108] The sorbent properties of polysulfide polymers, along with the presence of sulfur, suggest that they may serve as a viable support for AuNPs. Chalker and coworkers have utilised recycled cooking oil, in the presence of sodium chloride (NaCl) as a porogen, to synthesise a highly effective polysulfide sorbent material through inverse vulcanisation.[107,108] There are several methods to further increase the surface area and improve metal sorption into polymers, with carbonisation being the easiest and most scalable approach. This method has been used for polysulfide materials to enhance mercury sorption.[107] These polysulfide and carbonised polysulfide materials were synthesised as previously reported by Chalker and investigated as potential supports for AuNPs due to their high porosity and large surface area, making them suitable for gold deposition.[107,108]

Complete deposition of the AuNPs onto the polysulfide supports (10 g L^{-1}) was achieved by hydrazine hydrate (580 eq.) in $AuCl_4^-$ (20 ppm) model system (Table 1, entry 1). Similarly, 100% deposition was achieved with carbonised polysulfide materials (Table 1, entry 2) using 10 g L^{-1} of support with or without an external reductant, as determined by measuring the gold concentration of the solution by AAS. The ability to achieve less than 1% of gold remaining in the solution in the absence of an external reductant can be attributed to the polymer's sorbent properties and the reductive characteristics of sulfur-containing functional groups, particularly in the carbonised polysulfide material. Similarly, another polysulfide material derived from sulfur and cooking oil, using NaCl and urea as porogens, has been reported to exhibit both sorbent and reductive properties.[125] The sorbent nature of the resulting polymer was confirmed using XPS, which revealed the presence of gold in both metallic Au(0) and Au(III) salt forms on the support.[125]

Cellulose fibres were also investigated as an alternative support for AuNPs, achieving a 100% deposition yield (Table 1, entries 3 and 4). The highly crystalline structure of cellulose, resulting from extensive intermolecular and intramolecular hydrogen bonding, makes it insoluble in water and resistant to enzymatic degradation, establishing it as another viable support material.[126,127] Micronised cellulose (MCC) also appeared to be as suitable support (Table 1, entry 5). Carbonised cellulose fibres were also investigated as a support (Table 1, entry 6). Similar to the polysulfide and carbonised polysulfide materials, carbonised cellulose was able to remove all Au^{3+} salts from solution without an external reductant, likely due to the sorbent or self-reductive properties of the support. Although polysulfide, carbonised polysulfide, and carbonised cellulose fibres provide large surface areas for

Table 1 Deposition yields achieved with different supports and reductants. Deposition yields in parantheses were achieved with only the support without the use of an external reductant

Entry	Support	Reductant	Deposition yield (%)
1	Polysulfide	Hydrazine hydrate	100 (99)
2	Carbonised polysulfide	Hydrazine hydrate	100 (100)
3	Cellulose	Hydrazine hydrate	100
4	Cellulose	Ascorbic acid	100
5	Micronised cellulose	Hydrazine hydrate	100
6	Carbonised in-house charcoal	Hydrazine hydrate	100 (100)
7	Chitin	Ascorbic acid	32
8	Chitosan	Ascorbic acid	17
9	Starch	Ascorbic acid	73
10	Lecithin	Ascorbic acid	0

AuNP formation, their sorbent properties may leave salt precursors unreduced, making them less suitable as AuNP supports.

Chitin, in the form of microspheres, nanofibres, and nanogels, has previously been reported as a suitable support for AuNPs; therefore, it was also investigated as a support in this study.[123,128–131] Unmodified chitin was investigated as a potential support; however, it yielded a low Au deposition rate of 32% (Table 1, entry 7). Chitin is often further processed into nanocomposite materials, such as nanofibrils, nanofibres, microspheres, and mixed-ligand MOF nanosheets, which have been reported to achieve deposition rates of up to 99%.[123,129,132] Unmodified chitin has been reported to achieve a poor deposition of thiolate-capped Au nanoclusters.[133] Quantification of the residual gold in solution and the resulting Au wt% on chitin were not reported; however, the poor deposition was inferred from the observation of the remaining yellow solution, characteristic of Au chloride salt precursors.

Chitosan nanocomposite materials have been reported to be suitable AuNP supports.[124,134,135] In our study, unmodified chitosan was found to be a poor support material for AuNPs due to its solubility in acidic media and poor filtration properties (entry 8). Similar to chitin, chitosan requires pre-processing steps to become a viable support for AuNPs. Comparable solubility issues were observed with starch (Table 1, entry 9) and lecithin (Table 1, entry 10). Only a 73% deposition yield was achieved with starch, while lecithin showed a 0% deposition yield. The solubility issues of chitosan, starch, and lecithin rendered these materials impractical as solid supports.

Catalytic function

The catalytic performance of AuNPs loaded onto various supports was evaluated by measuring the rate of *p*-nitrophenol reduction. This reaction is notable for its simple experimental procedure and the ability to track progress using UV-vis spectroscopy, making it a common method for assessing the catalytic performance of nanoparticulate materials. Quantification is based on the decrease in absorbance intensity of *p*-nitrophenolate at 400 nm and the increase in absorbance at 290 nm, corresponding to the formation of *p*-aminophenolate. A typical procedure involved adding $NaBH_4$ (7.4 equivalents) to a solution of 4-NP in water, followed by the addition of AuNPs (20 mol%). Cellulose fibres proved to be the optimal support for catalytic activity, outperforming both polysulfide and carbonised polysulfide materials, achieving 98–100% conversion of *p*-nitrophenol within 90 minutes (Table 2, entry 1). Micronised cellulose was also tested and achieved 83% conversion within the same 90-minute timeframe (Table 2, entry 2). AuNPs loaded onto polysulfide support with hydrazine (Table 2, entry 3) and without hydrazine (Table 2, entry 4) as an external reductant did not exhibit any catalytic activity in the reduction of *p*-nitrophenol. The porous nature of the support may have resulted in AuNPs being embedded deep into the support, which is supported by the observation that it was difficult to characterise AuNPs using surface techniques such as SEM and XPS. Au(0) was confirmed by its

Table 2 Time-dependent reduction of *p*-nitrophenol by $NaBH_4$ using various supported AuNPs as catalysts. Yields in parentheses account for the residual solution and support extraction concentrations. All yields are based on triplicate experiments

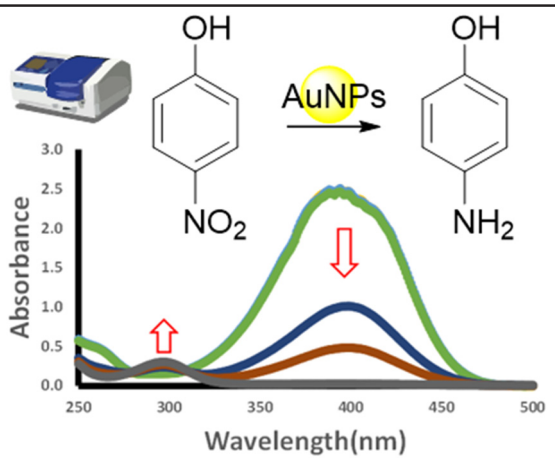

Entry	Support	4-NP reduction conversion yield (%)	k_{app} (min^{-1})
1	Cellulose	98–100	0.06
2	Micronised cellulose	83	0.01
3	Polysulfide (reductant used during catalyst synthesis)	0 (7)	—
4	Polysulfide (no reductant used during catalyst synthesis)	0	—
5	Carbonised polysulfide (reductant used during catalyst synthesis)	93 (50)	0.02
6	Carbonised polysulfide (no reductant used during catalyst synthesis)	81	0.04
7	Cellulose (trisodium citrate)	99	0.06

indicative XPS peaks at 84.6 eV and 88.1 eV, but the resulting spectra had much lower intensity that the Au spectra of the cellulose samples (S3, ESI†). With XPS, the path length of the photons are in the order of a few micrometres, but electrons are only in the order of tens of angstroms.[136] Ionisation occurs only at the depth of a few nm, and only these photoelectrons derived within tens of angstroms below the surface are able to exit the sample and contribute to the characteristic XPS peaks.[136] Thus, the surface limit of detection in XPS is 10 nm, and combined with the low spectral intensity of XPS and the inability to detect AuNPs using SEM, this suggests that the Au(0) is likely embedded deep within the polysulfide material.

The AuNPs stabilised on the carbonised polysulfide materials in the presence of an external reductant demonstrated the ability to reduce 4-NP (Table 2, entry 5). However, the carbonised polysulfide material had previously been shown to have sorbent properties for gold salt precursors, suggesting the possibility of absorbing organic compounds such as *p*-nitrophenolate. Control experiments using *p*-nitrophenol, $NaBH_4$, and polysulfide material in the absence of AuNPs revealed the ability of this system to absorb *p*-nitrophenolate from the solution. The catalytic function is determined by the residual substrate concentrations, which made assessing catalytic performance challenging in this case. An ethanol extract was performed on the material to determine the true conversion to 4-aminophenol. The polysulfide with AuNPs loaded with hydrazine hydrate only achieved a 7% conversion yield of *p*-nitrophenol when considering the residual concentration in the solution and the concentration washed off the support (Table 2, entry 3). Similarly, the carbonised polysulfide with AuNPs achieved 50% conversion (Table 2, entry 5). Due to the poor efficiency for the reduction of 4-NP using polysulfide- and carbonised polysulfide-stabilised AuNPs, combined with the uncertainty regarding whether the absorbed gold was in the reduced or salt form, materials synthesised without an external reductant were not pursued further. The possibility of incomplete reduction of gold salt precursors (Au(III) or Au(I)) to their nanoparticulate form (Au(0)) without an external reductant during catalyst synthesis was also the reason carbonised cellulose fibres were not further pursued.

Previously, trisodium citrate was shown to help stabilise the hydrodynamic size of generated AuNPs when using hydrazine hydrate as the external reductant. However, using trisodium citrate as the sole reductant was unsuccessful in achieving a high yield of gold deposition onto cellulose, reaching only a 20% yield. Therefore, it was not considered a suitable reductant. A 100% deposition yield was successfully achieved when a combination of trisodium citrate and hydrazine hydrate was used. Interestingly, when loaded onto cellulose, trisodium citrate combined with hydrazine hydrate performed as effectively as hydrazine hydrate alone. Both successfully reduced *p*-nitrophenol with a 98–99% yield, and the apparent kinetic rates were nearly identical (Table S1, ESI†). As a result, trisodium citrate was deemed not necessary to obtain stable AuNPs. Both unmodified and modified cellulose have previously been reported to be able to stabilise AuNPs.[47,48,52,137] A linear relationship between $\ln(A/A_o)$ and time (min) was observed, suggesting that the reaction followed pseudo-first-order kinetics. The pseudo-first-order rate constant (k_{app}) for the AuNP–cellulose catalysts was calculated to be 3.52 h^{-1} and 3.57 h^{-1} respectively for the $AuCl_4^-$ and AuI_4^- model systems (Table S3, ESI†). Despite these values not being as high as previously reported AuNPs (Table S3, ESI†), significant excess of $NaBH_4$ (up to 1588 eq.) and Au (up to 5000 mol%) are often used in these procedures which impact the reported kinetic values. Our standardised 4-NP reduction procedure uses only 7.4 molar equivalents of $NaBH_4$ and 20 mol% Au.

In addition to standardised 4-NP reduction comparison experiments, turnover number (TON, eqn (1)) and turnover frequency (TOF, eqn (2)) were also calculated using the following equations. The amount of product was determined based on the conversion of *p*-nitrophenolate at the end of the reaction, relative to the initial stock concentrations. The wt% of Au was measured by *aqua regia* digestion of the AuNP–cellulose samples.

$$\mathrm{TON} = \frac{n_{\mathrm{product}}}{n_{\mathrm{catalyst}}} \quad (1)$$

$$\mathrm{TOF} = \frac{\mathrm{TON}}{\mathrm{time}} \quad (2)$$

The TOF for the AuNP–cellulose catalysts were 795 h^{-1} and 1023 h^{-1} for the $AuCl_4^-$ and AuI_4^- precursor solutions, respectively, which outperforms or has similar efficiencies to AuNP–cellulose catalysts reported in the literature, which range from 0.1–1150 h^{-1} (Table 3).[46,47,52,138,139]

Table 3 TOF and TON from literature samples compared to this work

Entry	Sample description	TOF (h^{-1})	TON	Ref.
1	AuNPs on cellulose	260	—	46
		899	—	
		1198	—	
2	AuNPs on cellulose column	137	—	47
3	AuNPs on cellulose film	1150	—	52
4	AuNPs incorporated into cryogel walls	0.619	18.3	138
		0.073	1.92	
		0.365	5.74	
		0.255	5.14	
		0.071	1.72	
		0.066	1.40	
		0.087	2.11	
5	AuNPs stabilised by large-ring cyclodextrins	17	—	139
		29	—	
		34	—	
		43	—	
6	**$AuCl_4^-$ on cellulose**	**795**	**1330**	**This work**
7	**AuI_4^- on cellulose**	**1023**	**1744**	**This work**
8	**PCB e-waste sample**	**2713**	**6145**	**This work**

Characterisation of optimal AuNP catalysts

The final optimal catalysts for both the $AuCl_4^-$ or AuI_4^- model systems loaded onto cellulose were characterised using SEM, TEM, and XPS. Using TEM, 60–70% of the AuNPs were shown to be between the sizes of 0 to 10 nm for both model systems (Fig. 2B and C). With 70–80% of all AuNPs below 30 nm. Some larger clusters were also present.

All nanoparticles are in the form of Au(0), as the XPS spectra of all gold-loaded cellulose samples show only one species, with two spin–orbit split signals at 84.2 eV ($4f_{7/2}$) and 87.8 eV ($4f_{5/2}$). The Au $4f_{7/2}$ binding energy reference is at 84.00 eV (Δ = 3.7 eV), as depicted in Fig. 2A. If Au(I) and Au(III) salts were present, characteristic higher binding energies at 85.0 eV and 86.0 eV, respectively, would be observed.[140,141] The presence of metallic Au in the optimised catalyst is further confirmed by the absence of characteristic chloride or iodide peaks from the $AuCl_4^-$ or AuI_4^- source.

To further confirm the complete reduction of gold salts to Au(0) NPs on cellulose, a 1 L scale catalyst synthesis was performed using $AuCl_4^-$. AAS analysis of the stock solutions revealed a total of 19.51 mg of Au. A 100% deposition yield was achieved, as indicated by the solution falling below the detection limit. A sample of AuNPs on cellulose was digested with *aqua regia*, revealing a total Au content of 19.50 mg, with a ±0.06% error margin from the expected amount. Based on combined XPS and AAS analyses, it can be concluded that all precursor gold salts were successfully reduced to the Au(0) metallic state.

Effect of temperature during AuNP synthesis

The effect of temperature on nanoparticle (NP) formation and the catalytic function of AuNPs was also investigated. In the $AuCl_4^-$ model system, catalytic activity decreased as the synthesis temperature increased. TEM images revealed a reduction in the proportion of AuNPs smaller than 20 nm as the synthesis temperature rose. The optimal temperature for obtaining the largest proportion of AuNPs, ranging from 0 to 28 nm, was found to be room temperature (Table S1, ESI†). Given the importance of surface area in heterogeneous catalysis, it is proposed that the increase in particle size, caused by higher temperatures during catalyst synthesis, likely led to the observed decrease in 4-NP conversion (Fig. 3).

Interestingly, the AuI_4^- model system showed no significant effects with changes in temperature (Fig. 3). This is likely because the size distribution of the AuNPs remained largely unchanged across the different temperatures used for synthesis. Halide ions chemisorbed onto metal surfaces can also interact with Au with varying relative binding strengths.[142–145] The relative strength of Au-halide complexes decreases in the following order I > Br > Cl.[142–145] Iodide has been reported to greatly influence the resulting size and shape during AuNPs formation, and often induce aggregation.[146–149] However, both the $AuCl_4^-$ and AuI_4^- model systems have similar size and shape distribution factors. The resulting chloride and iodide concentrations from the initial 20 ppm stock solutions are comparable. The main difference between the two model systems lies in the initial pH and the pH during the deposition–reduction process. The initial pH of $AuCl_4^-$ remains close to 1 after the addition of hydrazine hydrate, while the pH of the AuI_4^- model system increases from approximately 5 to 10 after the addition of hydrazine hydrate. Various mechanistic and mathematical models have been developed for the widely used Turkevich synthesis, and there is a general consensus that the final size of the AuNPs is primarily influenced by the pH and the ratio of $[AuCl_4]^-$ to the less reactive $[AuCl_{3-x}(OH)_{1+x}]$ species. As the pH increases, OH^- ions progressively replace the Cl^- ligands, reducing the initial concentration of $AuCl_4^-$ available for seed particle formation.[150] However, the exact ratio of species can be various combinations of species, including $AuCl_4^-$ $AuCl_3(OH)^-$, $AuCl_2(OH)^{2-}$, $AuCl(OH)_3^-$, and $Au(OH)_4^-$.[151]

In the Turkevich model, temperature also influences the final size of the AuNPs by affecting the ratio of gold species, similarly to how changes in pH impact the synthesis.[150] UV-vis spectra showed that higher

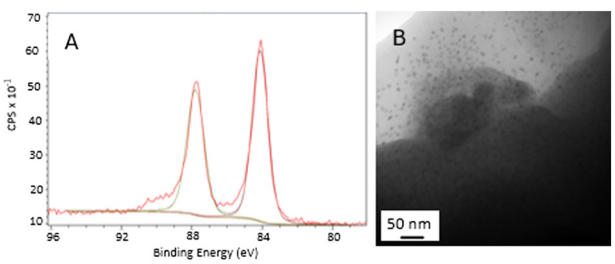

C	AuNP derived from AuI_4^- size distribution	AuNP derived from $AuCl_4^-$ size distribution
Size (nm)	%	%
3.0 – 28.3	72	87
28.3 – 53.6	15	13
53.6 – 78.9	8	-
78.9 – 104.2	2.5	-
104.2 – 129.5	2.5	*

Fig. 2 Characterisation of AuNPs on cellulose; (A) XPS spectra of AuNPs on cellulose. (B) TEM image of AuNPs from AuI_4^- model systems. (C) Size distribution of both AuI_4^- and $AuCl_4^-$ model systems. *Indistinguishable clusters present making it difficult to count (bottom).

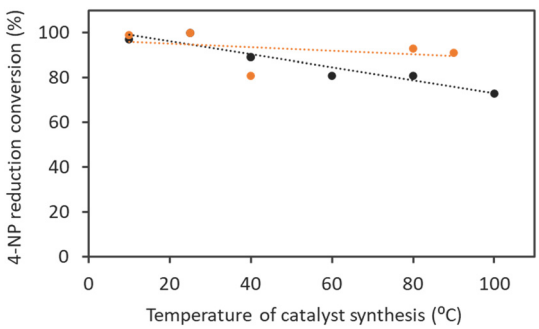

Fig. 3 Effect of catalyst synthesis temperature on the catalytic performance of AuNPs derived from the $AuCl_4^-$ (black) and AuI_4^- (orange) model systems.

temperatures favoured the formation of more hydroxylated gold species, leading to a decrease in Au(0) and a reduction in the number of particles.[150] Given the complexity of the reaction media, it is difficult to pinpoint the exact reason why the AuI_4^- model system is not impacted by temperature in the same way as the $AuCl_4^-$ system. This is especially true considering that the shape and size distributions are similar for both systems when synthesised under ambient conditions. Temperature likely influenced the ratio of Au-halide and $Au(OH)_x$ species more in the $AuCl_4^-$ system than in the AuI_4^- system, as the Au–I bond is stronger than the Au–Cl bond. This may explain why the $AuCl_4^-$ system was more sensitive to the increase in temperature during catalyst synthesis, leading to reduced catalytic efficiency compared to the AuI_4^- model system.

Comparison to commercial AuNPs and real-world e-waste-derived samples

Comparing catalytic activity with the existing literature is challenging due to the wide variation in reported reaction conditions. For example, the equivalents of $NaBH_4$ used vary significantly, ranging from 2 to 1588 molar equivalents. To benchmark our results, commercially available 30 nm AuNPs (stabilised in citrate buffer) were purchased and subjected to the same conditions to evaluate their catalytic function. The concentration of these AuNPs was first determined by digestion using *aqua regia*, giving a gold concentration of 36 ppm. Using the same gold molar equivalence of 0.2 and 7.4 molar equivalents of $NaBH_4$, identical to the SOP used for our model system, a conversion of 46% was observed (Table 4, entry 1), compared to the 98–100% conversion with the optimal model systems (Table 4, entries 2 and 3).

Several protocols have been reported highlighting the benefits of sodium citrate in the synthesis of monodisperse, quasi-spherical particles ranging from 10 to 300 nm.[152–155] However, while beneficial for the stability of the generated AuNPs, the presence of citrate can negatively affect their catalytic utility. Absorption studies of trisodium citrate on AuNPs in water have shown that the particles are coated with at least a monolayer of citrate molecules under both acidic and basic conditions.[156] The layer is based on the coordination of the absorbed citrate species to the AuNPs, and is almost exclusive bidentate and controlled by its protonation state.[157,158] This could in part explain the lower catalytic activity of the sample of commercially available AuNPs.

The stereoelectronic properties of the stabilising ligands on AuNPs including trisodium citrate have been shown to greatly impact the catalytic efficiency of 4-NP reduction by restructuring the AuNPs surface.[159–161] In the Langmuir–Hinshelwood (LH) model, ligand displacement by substrates on the AuNP surface is a dominant feature of the reaction mechanism. Borohydride ions react with the AuNP surface, leading to the formation of an AuNP-hydride species.[77,78] The presence of a monolayer of citrate molecules on the AuNP surface could have inhibited the adsorption of the reagents (*p*-nitrophenolate and borohydride ions) required for the reduction of *p*-nitrophenol. As a result, the commercially purchased AuNPs exhibited inferior catalytic activity compared to our cellulose–AuNPs synthesised from both model systems. This observation underscores that the choice of stabilising method—in our case, immobilising AuNPs onto cellulose—can significantly influence their catalytic efficiency and practical applicability.

The synthesis of AuNPs from PCB e-waste began with the removal of base metals using a combination of sulfuric acid and hydrogen peroxide, followed by a chloride-based gold-leaching process, before depositing the Au onto cellulose fibres.[93,102,162–166] TCCA was investigated as a gold-leaching reagent as it is a highly effective, low-cost, green and low-toxic leaching agent for gold ore and e-waste.[100,101,104,105,167–169] TCCA is also commonly used as a bleaching agent, disinfectant, and bactericide due to its oxidising and chlorinating properties, and is commercially available in pool supply and hardware stores.[170–172] It is also used in organic synthesis for the chlorination of aromatics, amines, amides, and carbonyls, as well as the oxidation of various functional groups.[170,171] The catalytic activity of the AuNPs derived from PCB e-waste samples using TCCA as a leachate was examined, and on all occasions, it outperformed all model samples having a significantly higher TOF and TON of 6145 and 2713 h^{-1}, respectively (Table 3, entry 8).

To determine why the e-waste-derived system outperformed the model systems, a full elemental analysis of the *aqua regia* digest of the generated catalyst was analysed using AAS and MP-AES (Table 5). The e-waste-derived sample was primarily composed of Au and residual base metals, including Fe, Mg, Al, and Pb. Corresponding XPS data also revealed the presence of Ag and possible trace amounts of Pd, which are likely responsible for the increased catalytic activity (Fig. 4). Palladium and silver nanoparticles have also been reported to be catalytic active for *p*-nitrophenol reduction.[173–176] The small quantities of Ag and Pd may help to explain the superior catalytic function of real-world e-waste samples. Surface imaging techniques such as SEM and TEM were also difficult when using materials derived from e-waste

Table 4 *p*-Nitrophenol yield reduction yield of our synthesised AuNPs from waste-derived concentrations compared to commercially available AuNPs

Entry	Sample description	Reductant	Temperature of catalyst synthesis	4-NP conversion yield (%)
1	Commercially available 30 nm AuNPs	N/A	N/A	46
2	$AuCl_4^-$ on cellulose	Hydrazine hydrate	RT	100
3	AuI_4^- on cellulose	Hydrazine hydrate	RT	100

Table 5 Metal compositions weight% of an e-waste-derived AuNP material on a cellulose support

Metal	wt%
Au	1.176
Pd	0.001
Al	0.049
Ca	0.000
Co	0.000
Cu	0.000
Fe	0.101
Mg	0.018
Mn	0.000
Ni	0.264
Pb	0.044
Sn	0.000
Zn	0.000

due to plastic and metal impurities. The AuNPs from model systems and e-waste-derived materials were also not uniformly distributed on the support. Various concentrations and surface screening were necessary for SEM and TEM imaging purposes. The non-uniform distribution of gold and impurities derived from e-waste also made XPS-surface-based techniques difficult. High-resolution XPS spectra were able to be obtained for C, O, and Au peaks of e-waste derived and model systems (Fig. 4). The HR-Au scan confirmed that Au existed solely as Au(0) as observed by the characteristic binding energy at 84.2 eV ($4f_{7/2}$) and 87.8 eV ($4f_{5/2}$).[140,141]

The HR-carbon scan of all the cellulose-based catalysts indicates the presence of lignin and fatty substances in the cellulose material, illustrated by the presence of C–C bond at 285 eV.[177] The e-waste-derived sample showed an additional peak at 290 eV, likely attributable to the O–C═O bond.[178] This could be due to commonly used plasticisers such as phthalate diesters, flame-retardants, and epoxy resin oxidised decomposition components,[179–183] but likely emanates from the oxidation of the primary alcohol of glucose to the carboxylic acid during the oxidative gold leaching conditions.

HR spectra of Ag 3d were obtained for e-waste-derived AuNPs from a chloride leach. The characteristic asymmetric signals for Ag 3d at 368.3 eV and 374.2 eV correspond to the $3d_{5/2}$ and $3d_{3/2}$ peaks, respectively. These values align with the well-separated spin–orbital components, with Δ = 6.0 eV and an observed spin–orbital splitting of 5.95 eV. However, it is challenging to determine whether the Ag present is in the form of metallic Ag(0) or Ag(I) (as AgCl). Typically, the composition of Ag is determined by the width of the peak, with Ag salts exhibiting broader peaks.[184,185] However, due to the low concentration and the absence of high-resolution chloride spectra, it is difficult to determine whether Ag is present as metallic AgNPs or AgCl. Palladium HR spectra of the e-waste-derived AuNPs were also obtained to provide evidence of the presence of palladium on the cellulose. Unfortunately, the characteristic asymmetric peak at 335 eV with a spin–orbital splitting (Δ = 5.26 eV) was not obtained. Due to the equivocal data derived from XPS to corroborate the presence of Pd, a different analysis technique was pursued. A PCB e-waste-derived cellulose–AuNP sample was ashed to concentrate the gold from a 22 g to a 0.6 g sample. The ashed material was then subjected to a fire assay involving a fusion process at 1200 °C that resulted in the formation of a lead-alloy bead that contains the desired precious group metals (PGMs). The resulting Pb-alloy bead was subjected to a cupellation at 900 °C to generate the final PGM bead containing Au, Ag, and Pd (Fig. 4). The resulting

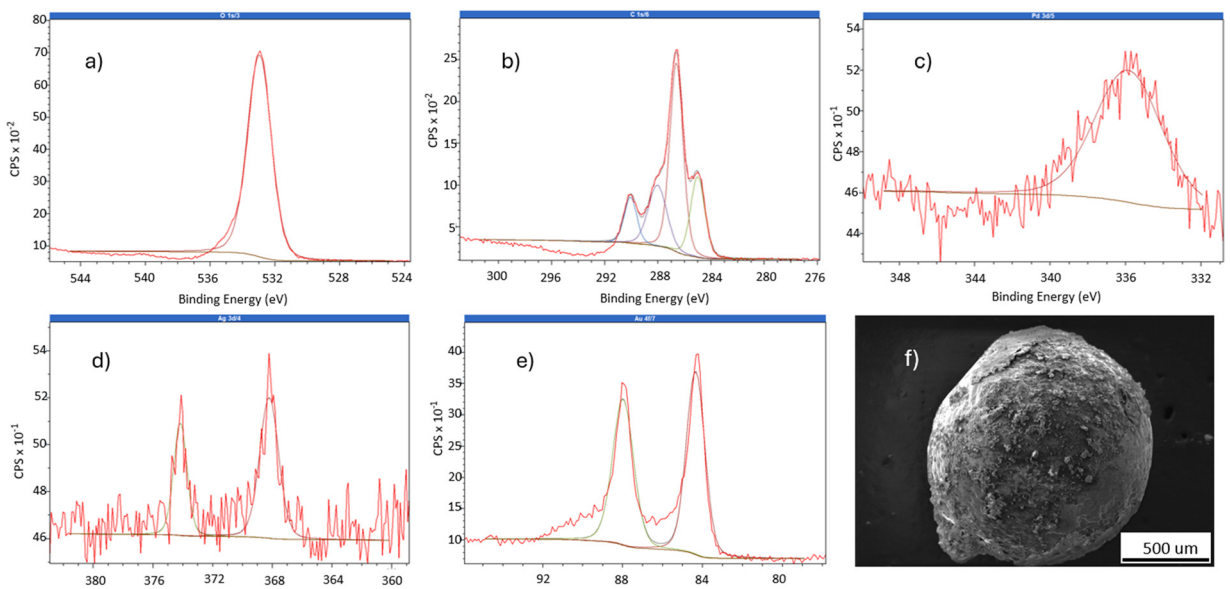

Fig. 4 a) HR-XPS O spectra of model systems and e-waste derived AuNPs. b) HR-XPS C spectra of model systems and e-waste derived AuNPs. c) HR-XPS Pd spectra of e-waste derived AuNPs. d) HR-XPS Ag spectra of e-waste derived AuNPs. e) HR-XPS spectra of e-waste derived AuNPs. f) SEM image of PGM alloy generated from electronic waste.

bead was initially analysed using EDS, but surface analysis was only able to determine the presence of Au and Ag, giving similar results to those previously obtained using XPS (Fig. S4, ESI†). Due to the heterogeneity of the sample and the limitations of surface techniques, a digestion was performed. The bead was rolled flat to facilitate three replicate digestions using *aqua regia*. Pd concentrations were analysed using AAS, revealing a Pd content of 0.13 wt% in the PGM alloy. The Pd content was then back-calculated to 0.0015 wt% on the cellulose support, approximately 950 times less than Au, which would help to explain the higher catalytic function of the e-waste-derived AuNPs. Other metals present on e-waste-derived samples include Al, Fe, Mg, Ni, and Pb, present in 0.049 wt%, 0.101 wt%, 0.018 wt%, and 0.264 wt% and 0.044 wt%, respectively. Of the metals present, only Ni and Fe have the potential to contribute to catalytic function, alongside Pd.[186–189] Given these trace quantities of catalytically active metals, strict protocols for using acid-washed glassware and equipment were followed to prevent contamination. Overall, the PCB e-waste-derived sample outperformed both model systems and commercially available AuNPs. This study demonstrates the practical feasibility of producing catalytically active AuNPs directly from waste-derived gold-containing solutions in the range of 20 to 30 ppm.

Conclusions

In summary, highly catalytically active AuNPs derived from PCB e-waste have been successfully reported. Through utilisation of a waste product, cellulose and the green oxidant TCCA, we have demonstrated the production of a high-value catalyst that shows superior performance to analogous AuNPs derived from stock gold solutions. Optimisation studies revealed hydrazine hydrate as the reductant, cellulose fibres as the support, and ambient conditions as best for for catalyst generation. The resulting AuNPs ranged in size from 3 to 30 nm, with the deposited Au exclusively in the Au(0) form, as determined by a combination of XPS and AAS. While considerable progress has been made in developing green methods for the production of AuNPs, most studies still rely on precursors refined from gold ore. E-waste is a rapidly growing global resource, and the ability to convert this waste into a catalytically useful material offers a greener and more sustainable alternative to traditional mining. However, several challenges remain. First, the heterogeneity of e-waste, typically classified into low, medium, and high grades, can result in significant variation in base and precious metal content. Second, the non-uniform distribution of gold and impurities in e-waste complicates characterisation using surface-based techniques. While these challenges exist, this study demonstrates the possibility to form catalytically useful AuNPs directly from leachate containing low concentrations of Au. This supports a circular economy and waste-utilisation of e-waste as a starting material, that will help minimise e-waste going into landfills and reduce need for mined gold. Often, e-waste is treated with pyrometallurgical involving incineration and further hydrometallurgical processes.[87,163] E-waste that is not recycled is often exported overseas to industrialised countries despite the Basel Ban.[190] An estimated 50–80% of the collected e-waste in the USA is not recycled domestically but shipped overseas.[190] Often, e-waste is labelled as second-hand goods, but the EU Commission estimates that 25–75% of these second-hand goods imported into Africa are broken and cannot be reused.[191] China processed 70% of the world's e-waste in 2012, with the remaining processed by India and other countries in eastern Asia and Africa.[192] By emphasising the value of e-waste products, a value-added process incentivises proper utilisation and recycling of e-waste. Future work will focus on the utility of waste-derived gold catalysts for hydrogenation, alkyne activation, oxidation and reductive coupling reactions.

Data availability

The data supporting this article have been included as part of the ESI.†

Author contributions

Michelle Lau: conceptualization, data curation, formal analysis, investigation, methodology, resources, writing – original draft, writing – review & editing. David C. Young: conceptualization, funding acquisition, investigation, project administration, supervision, writing – review & editing. Jack Chen: conceptualisation, supervision, investigation, writing – review & editing. Jonathan Sperry: conceptualisation, funding acquisition, investigation, project administration, supervision, writing – review & editing.

Conflicts of interest

The authors declare the following financial interests/personal relationships which may be considered as potential competing interests: Jonathan Sperry reports financial support was provided by University of Auckland. Michelle Lau reports financial support was provided by University of Auckland and Mint Innovation. David Young is employed by Mint Innovation, an e-waste recycling company. If there are other authors, they declare that they have no known competing financial interests or personal relationships that could have appeared to influence the work reported in this paper.

Acknowledgements

We thank the University of Auckland for the award of a Doctoral Scholarship (M. Y. L.) and Mint Innovation (NZ) for funding.

Notes and references

1 B. Hammer and J. K. Norskov, Why gold is the noblest of all the metals, *Nature*, 1995, **376**(6537), 238–240.

2 G. Baffou and R. Quidant, Nanoplasmonics for chemistry, *Chem. Soc. Rev.*, 2014, **43**(11), 3898.

3 T. Ishida, T. Murayama, A. Taketoshi and M. Haruta, Importance of Size and Contact Structure of Gold Nanoparticles for the Genesis of Unique Catalytic Processes, *Chem. Rev.*, 2020, **120**(2), 464–525.

4 M. Faraday, The Bakerian Lecture. —Experimental relations of gold (and other metals) to light, *Philos. Trans. R. Soc. London*, 1857, **147**, 145–181.

5 J. Turkevich, Colloidal gold. Part I: Historical and preparative aspects, morphology and structure, *Gold Bull.*, 1985, **18**(3), 86–91.

6 B. Nkosi, N. J. Coville, G. J. Hutchings, M. D. Adams, J. Friedl and F. E. Wagners, Hydrochlorination of acetylene using gold catalysts: A study of catalyst deactivation, *J. Catal.*, 1991, **128**(2), 366–377.

7 M. Haruta, T. Kobayashi, H. Sano and N. Yamada, Novel Gold Catalysts for the Oxidation of Carbon Monoxide at a Temperature far Below 0 °C, *Chem. Lett.*, 1987, **16**(2), 405–408.

8 C. Mohr, H. Hofmeister and P. Claus, The influence of real structure of gold catalysts in the partial hydrogenation of acrolein, *J. Catal.*, 2003, **213**(1), 86–94.

9 C. Mohr, H. Hofmeister, J. Radnik and P. Claus, Identification of Active Sites in Gold-Catalyzed Hydrogenation of Acrolein, *J. Am. Chem. Soc.*, 2003, **125**(7), 1905–1911.

10 R. Zanella, Crotonaldehyde hydrogenation by gold supported on TiO2: structure sensitivity and mechanism, *J. Catal.*, 2004, **223**(2), 328–339.

11 A. Corma and P. Serna, Chemoselective Hydrogenation of Nitro Compounds with Supported Gold Catalysts, *Science*, 2006, **313**(5785), 332–334.

12 P. Serna, P. Concepción and A. Corma, Design of highly active and chemoselective bimetallic gold–platinum hydrogenation catalysts through kinetic and isotopic studies, *J. Catal.*, 2009, **265**(1), 19–25.

13 A. Abad, A. Corma and H. García, Bridging the gap between homogeneous and heterogeneous gold catalysis: supported gold nanoparticles as heterogeneous catalysts for the benzannulation reaction, *Top. Catal.*, 2007, **44**(1–2), 237–243.

14 N. Anand, P. Ramudu, K. H. P. Reddy, K. S. R. Rao, B. Jagadeesh and V. S. P. Babu, *et al.*, Gold nanoparticles immobilized on lipoic acid functionalized SBA-15: Synthesis, characterization and catalytic applications, *Appl. Catal., A*, 2013, **454**, 119–126.

15 L. A. Aronica, E. Schiavi, C. Evangelisti, A. M. Caporusso, P. Salvadori and G. Vitulli, *et al.*, Solvated gold atoms in the preparation of efficient supported catalysts: Correlation between morphological features and catalytic activity in the hydrosilylation of 1-hexyne, *J. Catal.*, 2009, **266**(2), 250–257.

16 A. M. Caporusso, L. A. Aronica, E. Schiavi, G. Martra, G. Vitulli and P. Salvadori, Hydrosilylation of 1-hexyne promoted by acetone solvated gold atoms derived catalysts, *J. Organomet. Chem.*, 2005, **690**(4), 1063–1066.

17 S. Carrettin, M. C. Blanco, A. Corma and A. S. K. Hashmi, Heterogeneous Gold-Catalysed Synthesis of Phenols, *Adv. Synth. Catal.*, 2006, **348**(10–11), 1283–1288.

18 L. L. Chng, J. Yang, Y. Wei and J. Y. Ying, Semiconductor-Gold Nanocomposite Catalysts for the Efficient Three-Component Coupling of Aldehyde, Amine and Alkyne in Water, *Adv. Synth. Catal.*, 2009, **351**(17), 2887–2896.

19 K. K. R. Datta, B. V. S. Reddy, K. Ariga and A. Vinu, Gold Nanoparticles Embedded in a Mesoporous Carbon Nitride Stabilizer for Highly Efficient Three-Component Coupling Reaction, *Angew. Chem., Int. Ed.*, 2010, **49**(34), 5961–5965.

20 M. Kidwai, V. Bansal, A. Kumar and S. Mozumdar, The first Au-nanoparticles catalyzed green synthesis of propargylamines via a three-component coupling reaction of aldehyde, alkyne and amine, *Green Chem.*, 2007, **9**(7), 742.

21 V. Kotzabasaki, I. N. Lykakis, C. Gryparis, A. Psyllaki, E. Vasilikogiannaki and M. Stratakis, Gold-Catalyzed Dehydrogenative Cycloaddition of Tethered 1, *n*-Dihydrodisilanes to Alkynes, *Organometallics*, 2013, **32**(2), 665–672.

22 A. Leyva-Pérez, J. Oliver-Meseguer, J. R. Cabrero-Antonino, P. Rubio-Marqués, P. Serna and S. I. Al-Resayes, *et al.*, Reactivity of Electron-Deficient Alkynes on Gold Nanoparticles, *ACS Catal.*, 2013, **3**(8), 1865–1873.

23 I. N. Lykakis, A. Psyllaki and M. Stratakis, Oxidative Cycloaddition of 1,1,3,3-Tetramethyldisiloxane to Alkynes Catalyzed by Supported Gold Nanoparticles, *J. Am. Chem. Soc.*, 2011, **133**(27), 10426–10429.

24 S. Alabbad, S. F. Adil, M. E. Assal, M. Khan, A. Alwarthan and M. R. H. Siddiqui, Gold & silver nanoparticles supported on manganese oxide: Synthesis, characterization and catalytic studies for selective oxidation of benzyl alcohol, *Arabian J. Chem.*, 2014, **7**(6), 1192–1198.

25 N. Dimitratos, A. Villa, D. Wang, F. Porta, D. Su and L. Prati, Pd and Pt catalysts modified by alloying with Au in the selective oxidation of alcohols, *J. Catal.*, 2006, **244**(1), 113–121.

26 J. Han, Y. Liu and R. Guo, Reactive Template Method to Synthesize Gold Nanoparticles with Controllable Size and Morphology Supported on Shells of Polymer Hollow Microspheres and Their Application for Aerobic Alcohol Oxidation in Water, *Adv. Funct. Mater.*, 2009, **19**(7), 1112–1117.

27 J. Hu, L. Chen, K. Zhu, A. Suchopar and R. Richards, Aerobic oxidation of alcohols catalyzed by gold nanoparticles confined in the walls of mesoporous silica, *Catal. Today*, 2007, **122**(3–4), 277–283.

28 M. N. Hughes and H. G. Nicklin, Autoxidation of hydroxylamine in alkaline solutions, *J. Chem. Soc. A*, 1971, **164**, 3485–3487.

29 Y. Liu, H. Tsunoyama, T. Akita and T. Tsukuda, Preparation of ~1 nm Gold Clusters Confined within Mesoporous Silica and Microwave-Assisted Catalytic Application for Alcohol Oxidation, *J. Phys. Chem. C*, 2009, **113**(31), 13457–13461.

30 F. Su, Y. Liu, L. Wang, Y. Cao, H. He and K. Fan, Ga–Al Mixed-Oxide-Supported Gold Nanoparticles with Enhanced Activity for Aerobic Alcohol Oxidation, *Angew. Chem., Int. Ed.*, 2008, **47**(2), 334–337.

31 F. Z. Su, M. Chen, L. C. Wang, X. S. Huang, Y. M. Liu and Y. Cao, *et al.*, Aerobic oxidation of alcohols catalyzed by gold nanoparticles supported on gallia polymorphs, *Catal. Commun.*, 2008, **9**(6), 1027–1032.

32 L. C. Wang, Y. M. Liu, M. Chen, Y. Cao, H. Y. He and K. N. Fan, MnO_2 Nanorod Supported Gold Nanoparticles with Enhanced Activity for Solvent-free Aerobic Alcohol Oxidation, *J. Phys. Chem. C*, 2008, **112**(17), 6981–6987.

33 C. González-Arellano, A. Abad, A. Corma, H. García, M. Iglesias and F. Sánchez, Catalysis by Gold(I) and Gold(III): A Parallelism between Homo- and Heterogeneous Catalysts for Copper-Free Sonogashira Cross-Coupling Reactions, *Angew. Chem., Int. Ed.*, 2007, **46**(9), 1536–1538.

34 J. Han, Y. Liu and R. Guo, Facile Synthesis of Highly Stable Gold Nanoparticles and Their Unexpected Excellent Catalytic Activity for Suzuki–Miyaura Cross-Coupling Reaction in Water, *J. Am. Chem. Soc.*, 2009, **131**(6), 2060–2061.

35 V. K. Kanuru, G. Kyriakou, S. K. Beaumont, A. C. Papageorgiou, D. J. Watson and R. M. Lambert, Sonogashira Coupling on an Extended Gold Surface in Vacuo: Reaction of Phenylacetylene with Iodobenzene on Au(111), *J. Am. Chem. Soc.*, 2010, **132**(23), 8081–8086.

36 B. Karimi and F. Kabiri Esfahani, Unexpected golden Ullmann reaction catalyzed by Au nanoparticles supported on periodic mesoporous organosilica (PMO), *Chem. Commun.*, 2011, **47**(37), 10452.

37 G. Kyriakou, S. K. Beaumont, S. M. Humphrey, C. Antonetti and R. M. Lambert, Sonogashira Coupling Catalyzed by Gold Nanoparticles: Does Homogeneous or Heterogeneous Catalysis Dominate?, *ChemCatChem*, 2010, **2**(11), 1444–1449.

38 K. Layek, H. Maheswaran and M. L. Kantam, Ullmann coupling of aryl iodides catalyzed by gold nanoparticles stabilized on nanocrystalline magnesium oxide, *Catal. Sci. Technol.*, 2013, **3**(4), 1147.

39 M. Palashuddin Sk, C. K. Jana and A. Chattopadhyay, A gold–carbon nanoparticle composite as an efficient catalyst for homocoupling reaction, *Chem. Commun.*, 2013, **49**(74), 8235.

40 H. Tsunoyama, H. Sakurai, N. Ichikuni, Y. Negishi and T. Tsukuda, Colloidal Gold Nanoparticles as Catalyst for Carbon–Carbon Bond Formation: Application to Aerobic Homocoupling of Phenylboronic Acid in Water, *Langmuir*, 2004, **20**(26), 11293–11296.

41 H.-x. Wang, C.-b. Sun, S.-y. Li, P.-f. Fu, Y.-g. Song and L. Li, *et al.*, Study on gold concentrate leaching by iodine-iodide, *Int. J. Miner., Metall. Mater.*, 2013, **20**(4), 323–328.

42 N. Zhang, H. Qiu, Y. Liu, W. Wang, Y. Li and X. Wang, *et al.*, Fabrication of gold nanoparticle/graphene oxide nanocomposites and their excellent catalytic performance, *J. Mater. Chem.*, 2011, **21**(30), 11080.

43 V. Voliani, *Gold nanoparticles: an introduction to synthesis, properties and applications*, De Gruyter, Berlin Boston, 2020, p. 103.

44 P. Suchomel, L. Kvitek, R. Prucek, A. Panacek, A. Halder and S. Vajda, *et al.*, Simple size-controlled synthesis of Au nanoparticles and their size-dependent catalytic activity, *Sci. Rep.*, 2018, **8**(1), 4589.

45 M. Luty-Błocho, M. Wojnicki and K. Fitzner, Gold Nanoparticles Formation via Au(III) Complex Ions Reduction with L-Ascorbic Acid, *Int. J. Chem. Kinet.*, 2017, **49**(11), 789–797.

46 M. Chen, H. Kang, Y. Gong, J. Guo, H. Zhang and R. Liu, Bacterial Cellulose Supported Gold Nanoparticles with Excellent Catalytic Properties, *ACS Appl. Mater. Interfaces*, 2015, **7**(39), 21717–21726.

47 Md. T. Islam, J. E. Padilla, N. Dominguez, D. C. Alvarado, M. S. Alam and P. Cooke, *et al.*, Green synthesis of gold nanoparticles reduced and stabilized by squaric acid and supported on cellulose fibers for the catalytic reduction of 4-nitrophenol in water, *RSC Adv.*, 2016, **6**(94), 91185–91191.

48 J. Hwang, A. B. Siddique, Y. J. Kim, H. Lee, J. H. Maeng and Y. Ahn, *et al.*, Ionic cellulose-stabilized gold nanoparticles and their application in the catalytic reduction of 4-nitrophenol, *RSC Adv.*, 2018, **8**(4), 1758–1763.

49 Y. S. Seo, E. Y. Ahn, J. Park, T. Y. Kim, J. E. Hong and K. Kim, *et al.*, Catalytic reduction of 4-nitrophenol with gold nanoparticles synthesized by caffeic acid, *Nanoscale Res. Lett.*, 2017, **12**(1), 7.

50 K. Kuroda, T. Ishida and M. Haruta, Reduction of 4-nitrophenol to 4-aminophenol over Au nanoparticles deposited on PMMA, *J. Mol. Catal. A: Chem.*, 2009, **298**(1–2), 7–11.

51 T. Ma, W. Yang, S. Liu, H. Zhang and F. Liang, A Comparison Reduction of 4-Nitrophenol by Gold Nanospheres and Gold Nanostars, *Catalysts*, 2017, **7**(12), 38.

52 C. R. Cabreira and F. F. Camilo, Evaluation of catalytic activity of cellulose films decorated with gold nanoparticles in the reduction of 4-nitrophenol, *Cellulose*, 2020, **27**(7), 3919–3929.

53 M. Abd Elkodous, H. M. El-Husseiny, G. S. El-Sayyad, A. H. Hashem, A. S. Doghish and D. Elfadil, *et al.*, Recent advances in waste-recycled nanomaterials for biomedical applications: Waste-to-wealth, *Nanotechnol. Rev.*, 2021, **10**(1), 1662–1739.

54 M. Meena Kumari and D. Philip, Facile one-pot synthesis of gold and silver nanocatalysts using edible coconut oil, *Spectrochim. Acta, Part A*, 2013, **111**, 154–160.

55 B. Yang, F. Qi, J. Tan, T. Yu and C. Qu, Study of Green Synthesis of Ultrasmall Gold Nanoparticles Using Citrus Sinensis Peel, *Appl. Sci.*, 2019, **9**(12), 2423.

56 L. Castro, M. L. Blázquez, F. González, J. A. Muñoz and A. Ballester, Gold, Silver and Platinum Nanoparticles Biosynthesized Using Orange Peel Extract, *Adv. Mater. Res.*, 2013, **825**, 556–559.

57 C. Yuan, C. Huo, B. Gui and W. Cao, Green synthesis of gold nanoparticles using *Citrus maxima* peel extract and their catalytic/antibacterial activities, *IET Nanobiotechnol.*, 2017, **11**(5), 523–530.

58 A. Bankar, B. Joshi, A. Ravi Kumar and S. Zinjarde, Banana peel extract mediated synthesis of gold nanoparticles, *Colloids Surf., B*, 2010, **80**(1), 45–50.

59 G. K. Deokar and A. G. Ingale, Green synthesis of gold nanoparticles (Elixir of Life) from banana fruit waste extract – an efficient multifunctional agent, *RSC Adv.*, 2016, **6**(78), 74620–74629.

60 W. Chums-ard, D. Fawcett, C. C. Fung and G. E. J. Poinern, Biogenic synthesis of gold nanoparticles from waste watermelon and their antibacterial activity against Escherichia coli and Staphylococcus epidermidis, *Int. J. Res. Med. Sci.*, 2019, **7**(7), 2499.

61 A. E. Adebayo, A. M. Oke, A. Lateef, A. A. Oyatokun, O. D. Abisoye and I. P. Adiji, *et al.*, Biosynthesis of silver, gold and silver–gold alloy nanoparticles using Persea americana fruit peel aqueous extract for their biomedical properties, *Nanotechnol. Environ. Eng.*, 2019, **4**(1), 13.

62 N. German, A. Ramanavicius and A. Ramanaviciene, Electrochemical deposition of gold nanoparticles on graphite rod for glucose biosensing, *Sens. Actuators, B*, 2014, **203**, 25–34.

63 A. R. Sadrolhosseini, S. Abdul Rashid and A. Zakaria, Synthesis of Gold Nanoparticles Dispersed in Palm Oil Using Laser Ablation Technique, *J. Nanomater.*, 2017, **2017**, 1–5.

64 R. Sharma, N. F. Suhendra, S. H. Jung and H.-i Lee, Gold recovery at ultra-high purity from electronic waste using selective polymeric film, *Chem. Eng. J.*, 2023, **451**, 138506.

65 T. S. Nguyen, Y. Hong, N. A. Dogan and C. T. Yavuz, Gold Recovery from E-Waste by Porous Porphyrin–Phenazine Network Polymers, *Chem. Mater.*, 2020, **32**(12), 5343–5349.

66 R. Sharma, S. N. Chavan and H.-i. Lee, Fluorescent imidazolium hydrogels for tracing and recovering platinum with highest purity from spent auto catalyst, *Sens. Actuators, B*, 2023, **396**, 134625.

67 Y. J. Park and D. J. Fray, Recovery of high purity precious metals from printed circuit boards, *J. Hazard. Mater.*, 2009, **164**(2–3), 1152–1158.

68 H. Moriwaki, K. Yamada and H. Usami, Electrochemical extraction of gold from wastes as nanoparticles stabilized by phospholipids, *Waste Manage.*, 2017, **60**, 591–595.

69 S. Das, B. Dong and Y. P. Ting, Gold Biodissolution from Electronic Scrap and Biomineralization of Bacterial Gold Nanoparticles, *Adv. Mater. Res.*, 2015, **1130**, 668–672.

70 A. Nobahar, J. P. Lourenço, M. C. Costa and J. D. Carlier, Printed Circuit Boards Leaching Followed by Synthesis of Gold Nanoparticle Clusters Using Plant Extracts, *Waste Biomass Valoriz.*, 2024, **15**(4), 1999–2017.

71 A. Demirbas, K. Büyükbezirci, C. Celik, E. Kislakci, Z. Karaagac and E. Gokturk, *et al.*, Synthesis of Long-Term Stable Gold Nanoparticles Benefiting from Red Raspberry (*Rubus idaeus*), Strawberry (*Fragaria ananassa*), and Blackberry (*Rubus fruticosus*) Extracts–Gold Ion Complexation and Investigation of Reaction Conditions, *ACS Omega*, 2019, **4**(20), 18637–18644.

72 M. Baruch-Soto, L. Magallón-Cacho, J. Ramírez-Aparicio, J. Ortega-Guzmán and E. Borja-Arco, Methanol Oxidation Reaction in Alkaline Media Using Gold Nanoparticles Recovered from Electronic Waste, *Materials*, 2024, **17**(6), 1267.

73 G. J. Su, R. V. Maturano, R. Zanella and A. E. J. Borja, Turning trash into treasure: Gold nanoparticles (from e-waste) supported on TiO2 as catalyst for the oxidation of CO, *Nano-Struct. Nano-Objects*, 2024, **39**, 101235.

74 R. Sharma, Y. Kim, E. Lee and H.-i. Lee, Ultrapure gold recovery from electronic waste as nanoparticles immobilized in hydrogel matrix, *Chem. Eng. J.*, 2024, **499**, 156539.

75 W. Wang, W. Xue, Z. Huang, Z. Fang, T. Yan and X. Zhao, *et al.*, Harvesting low-cost gold-based catalysts from e-waste by a cationic covalent triazine organic framework for 4-nitrophenol reduction, *Chem. Eng. J.*, 2024, **499**, 156667.

76 S. McCarthy, O. Desaunay, A. L. W. Jie, M. Hassatzky, A. J. P. White and P. Deplano, *et al.*, Homogeneous Gold Catalysis Using Complexes Recovered from Waste Electronic Equipment, *ACS Sustainable Chem. Eng.*, 2022, **10**(48), 15726–15734.

77 S. Wunder, Y. Lu, M. Albrecht and M. Ballauff, Catalytic Activity of Faceted Gold Nanoparticles Studied by a Model Reaction: Evidence for Substrate-Induced Surface Restructuring, *ACS Catal.*, 2011, **1**(8), 908–916.

78 S. Wunder, F. Polzer, Y. Lu, Y. Mei and M. Ballauff, Kinetic Analysis of Catalytic Reduction of 4-Nitrophenol by Metallic Nanoparticles Immobilized in Spherical Polyelectrolyte Brushes, *J. Phys. Chem. C*, 2010, **114**(19), 8814–8820.

79 B. Ramesh Babu, A. Kuber and C. Ahmed, Electrical and electronic waste: a global environmental problem, *Waste Manage. Res.*, 2007, **25**(4), 307–318.

80 R. Widmer, H. Oswald-Krapf, D. Sinha-Khetriwal, M. Schnellmann and H. Böni, Global perspectives on e-waste, *Environ. Impact Assess. Rev.*, 2005, **25**(5), 436–458.

81 H. Ghimire and P. A. Ariya, E-Wastes: Bridging the Knowledge Gaps in Global Production Budgets, Composition, Recycling and Sustainability Implications, *Sustainable Chem.*, 2020, **1**(2), 154–182.

82 B. Ghosh, M. K. Ghosh, P. Parhi, P. S. Mukherjee and B. K. Mishra, Waste Printed Circuit Boards recycling: an extensive assessment of current status, *J. Cleaner Prod.*, 2015, **94**, 5–19.

83 W. He, G. Li, X. Ma, H. Wang, J. Huang and M. Xu, *et al.*, WEEE recovery strategies and the WEEE treatment status in China, *J. Hazard. Mater.*, 2006, **136**(3), 502–512.

84 **https://www.mint.bio/**.

85 P. H. Brunner, Urban Mining A Contribution to Reindustrializing the City, *J. Ind. Ecol.*, 2011, **15**(3), 339–341.

86 B. Sceresini, Gold-copper ores, in *Developments in Mineral Processing*, Elsevier, 2005, pp. 789–824.

87 A. Golev, G. D. Corder and M. A. Rhamdhani, Estimating flows and metal recovery values of waste printed circuit boards in Australian e-waste, *Miner. Eng.*, 2019, **137**, 171–176.

88 L. Pietrelli, S. Ferro and M. Vocciante, Eco-friendly and cost-effective strategies for metals recovery from printed circuit boards, *Renewable Sustainable Energy Rev.*, 2019, **112**, 317–323.

89 P. P. Sheng and T. H. Etsell, Recovery of gold from computer circuit board scrap using aqua regia, *Waste Manage. Res.*, 2007, **25**(4), 380–383.

90 D. Silvana, V. Trujic and I. Aleksandra, Recycling of precious metal from e-scrap, *Iran. J. Chem. Chem. Eng.*, 2013, **32**(4), 17–23.

91 B. Altansukh, K. Haga, H. H. Huang and A. Shibayama, Gold Recovery from Waste Printed Circuit Boards by Advanced Hydrometallurgical Processing, *Mater. Trans.*, 2019, **60**(2), 287–296.

92 Q. Xu and D. Chen, Iodine leaching process for recovery of gold from waste PCB, *Huanjing Gongcheng Xuebao*, 2009, **3**(5), 911–914.

93 B. Lucheva, P. Iliev and D. Kolev, Recovery of gold from electronic waste by iodine-iodide leaching, *J. Chem. Technol. Metall.*, 2017, **52**(2), 322–326.

94 M. Sahin, A. Akcil, C. Erust, S. Altynbek, C. S. Gahan and A. Tuncuk, A Potential Alternative for Precious Metal Recovery from E-waste: Iodine Leaching, *Sep. Sci. Technol.*, 2015, **50**, 2587–2595.

95 C. O. Calgaro, D. F. Schlemmer, M. D. C. R. Da Silva, E. V. Maziero, E. H. Tanabe and D. A. Bertuol, Fast copper extraction from printed circuit boards using supercritical carbon dioxide, *Waste Manage.*, 2015, **45**, 289–297.

96 P. A. Olubambi and J. H. Potgieter, Investigations on the mechanisms of sulfuric acid leaching of chalcopyrite in the presence of hydrogen peroxide, *Miner. Process. Extr. Metall. Rev.*, 2009, **30**(4), 327–345.

97 J. Rajahalme, S. Perämäki, R. Budhathoki and A. Väisänen, Effective Recovery Process of Copper from Waste Printed Circuit Boards Utilizing Recycling of Leachate, *JOM*, 2021, **73**(4), 980–987.

98 D. Salas-Martell, G. Pareja-Guzman, J. Tello-Hijar and J. C. F. Rodriguez-Reyes, Leaching of a pyrite-based ore containing copper using sulfuric acid and hydrogen peroxide, *Int. J. Ind. Chem.*, 2020, **11**(3), 195–201.

99 M. Kumar, J.-c. Lee, M. S. Kim and J. Jeong, Leaching of metals from waste printed circuit boards (WPCBs) using sulfuric and nitric acids, *Environ. Eng. Manage. J.*, 2014, **13**(10), 2601–2607.

100 Q. Li, Y. Huang, Z. Xiong and R. Zha, New Organic Leaching and Recycling of Gold, Nickel, and Copper in Waste Printed Circuit Boards, in *Proceedings of the 15th International Conference on Waste Management and Technology*, 2020.

101 J. Wordsworth, N. Khan, J. Blackburn, J. E. Camp and A. Angelis-Dimakis, Technoeconomic Assessment of Organic Halide Based Gold Recovery from Waste Electronic and Electrical Equipment, *Resources*, 2021, **10**(17), 1–12.

102 J. M. Chalker and M. Mann, Materials and processes for recovering precious metals, PCT, WO2020198778A1, 2020.

103 J. M. Chalker and M. J. H. Worthington, Metal Adsorbent Material and Uses Thereof, PCT, WO2017181217A1, 2017.

104 H. Niu, Research on gold leaching of carbonaceous pressure-oxidized gold ore via a highly effective, green and low toxic agent trichloroisocyanuric acid, *J. Cleaner Prod.*, 2023, **419**, 138062.

105 B. K. Kenzhaliyev, N. K. Tussupbayev, G. Z. Abdykirova, A. K. Koizhanova, D. Y. Fischer and Z. A. Baltabekova, Evaluation of the Efficiency of Using an Oxidizer in the Leaching Process of Gold-Containing Concentrate, *Processes*, 2024, **6**, 598.

106 L. Huang, Mechanical activation and characterization of micronized cellulose particles from pulp fiber, *Ind. Crops Prod.*, 2019, **141**, 11750.

107 M. Mann, X. Luo, A. D. Tikoalu, C. T. Gibson, Y. Yin and R. Al-Attabi, *et al.*, Carbonisation of a polymer made from sulfur and canola oil, *Chem. Commun.*, 2021, **57**(51), 6296–6299.

108 F. G. Müller, L. S. Lisboa and J. M. Chalker, Inverse Vulcanized Polymers for Sustainable Metal Remediation, *Adv. Sustainable Syst.*, 2023, **7**(5), 2300010.

109 X. Wang, P. Ou, A. Ozden, S. F. Hung, J. Tam and C. M. Gabardo, *et al.*, Efficient electrosynthesis of n-propanol from carbon monoxide using a Ag–Ru–Cu catalyst, *Nat. Energy*, 2022, **7**(2), 170–176.

110 S. Nam, M. Easson, J. H. Jordan, Z. He, H. Zhang and M. Santiago Cintrón, *et al.*, Unveiling the Hidden Value of Cotton Gin Waste: Natural Synthesis and Hosting of Silver Nanoparticles, *ACS Omega*, 2023, **8**(34), 31281–31292.

111 Y. Wei, W. Zhang and J. Gao, Trash or treasure? Sustainable noble metal recovery, *Green Chem.*, 2024, **26**, 5684–5707.

112 P. Pati, S. McGinnis and P. J. Vikesland, Waste not want not: life cycle implications of gold recovery and recycling from nanowaste, *Environ. Sci.: Nano*, 2016, **3**(5), 1133–1143.

113 U. Jadhav and H. Hocheng, Hydrometallurgical Recovery of Metals from Large Printed Circuit Board Pieces, *Sci. Rep.*, 2015, **5**(1), 14574.

114 S. M. Saleh, S. A. Said and M. S. El-Shahawi, Extraction and recovery of Au, Sb and Sn from electrorefined solid waste, *Anal. Chim. Acta*, 2001, **436**(1), 69–77.

115 G. Mishra, R. Jha, M. D. Rao, A. Meshram and K. K. Singh, Recovery of silver from waste printed circuit boards (WPCBs) through hydrometallurgical route: A review, *Environ. Challenges*, 2021, **4**, 100073.

116 V. S. Kogan and I. V. Berkovich, Silver, gold and palladium leaching from electronic scrap using bromine- bromide solution, *Kompleksnoe Ispolzovanie Mineralnogo Syra = Complex Use of Mineral Resources*, 2019, **311**(4), 35–47.

117 I. Birloaga, V. Coman, B. Kopacek and F. Vegliò, An advanced study on the hydrometallurgical processing of waste computer printed circuit boards to extract their valuable content of metals, *Waste Manage.*, 2014, **34**(12), 2581–2586.

118 V. H. Ha, J.-c. Lee, J. Jeong, H. T. Hai and M. K. Jha, Thiosulfate leaching of gold from waste mobile phones, *J. Hazard. Mater.*, 2010, **178**(1–3), 1115–1119.

119 M. Gurung, B. B. Adhikari, X. Gao, S. Alam and K. Inoue, Sustainability in the Metallurgical Industry: Chemically Modified Cellulose for Selective Biosorption of Gold from Mixtures of Base Metals in Chloride Media, *Ind. Eng. Chem. Res.*, 2014, **53**(20), 8565–8576.

120 J. Turkevich, P. C. Stevenson and J. Hillier, A study of the nucleation and growth processes in the synthesis of colloidal gold, *Discuss. Faraday Soc.*, 1951, **11**, 55.

121 D. Astruc, F. Lu and J. R. Aranzaes, Nanoparticles as Recyclable Catalysts: The Frontier between Homogeneous and Heterogeneous Catalysis, *Angew. Chem., Int. Ed.*, 2005, **44**(48), 7852–7872.

122 S. Kamel, Recent advances in cellulose supported metal nanoparticles as green and sustainable catalysis for organic synthesis, *Cellulose*, 2021, **28**, 4545–4574.

123 Y. Huang, Y. Fang, L. Chen, A. Lu and L. Zhang, One-step synthesis of size-tunable gold nanoparticles immobilized on chitin nanofibrils via green pathway and their potential applications, *Chem. Eng. J.*, 2017, **315**, 573–582.

124 C. O. Mohan, S. Gunasekaran and C. N. Ravishankar, Chitosan-capped gold nanoparticles for indicating temperature abuse in frozen stored products, *npj Sci. Food*, 2019, **3**(1), 2.

125 Z. Ren, X. Jiang, L. Liu, C. Yin, S. Wang and X. Yang, Modification of high-sulfur polymer using a mixture porogen and its application as advanced adsorbents for Au(III) from wastewater, *J. Mol. Liq.*, 2021, **328**, 115437.

126 A. Zoghlami and G. Paës, Lignocellulosic Biomass: Understanding Recalcitrance and Predicting Hydrolysis, *Front. Chem.*, 2019, **7**, 874.

127 A. T. W. M. Hendriks and G. Zeeman, Pretreatments to enhance the digestibility of lignocellulosic biomass, *Bioresour. Technol.*, 2009, **100**(1), 10–18.

128 T. Naghdi, H. Golmohammadi, H. Yousefi, M. Hosseinifard, U. Kostiv and D. Horák, *et al.*, Chitin Nanofiber Paper toward Optical (Bio)sensing Applications, *ACS Appl. Mater. Interfaces*, 2020, **12**(13), 15538–15552.

129 Y. Wang, Y. Li, S. Liu and B. Li, Fabrication of chitin microspheres and their multipurpose application as catalyst support and adsorbent, *Carbohydr. Polym.*, 2015, **120**, 53–59.

130 J. Zhang, W. Zhu, J. Liang, L. Li, L. Zheng and X. Shi, *et al.*, In Situ Synthesis of Gold Nanoparticles from Chitin Nanogels and Their Drug Release Response to Stimulation, *Polymer*, 2024, **16**(3), 390.

131 Z. Shervani, Y. Taisuke, S. Ifuku, H. Saimoto and M. Morimoto, Preparation of Gold Nanoparticles Loaded Chitin Nanofiber Composite, *Adv. Nanopart.*, 2012, **01**(03), 71–78.

132 R. Yan, Y. Zhao, H. Yang, X. Kang, C. Wang and L. Wen, *et al.*, Ultrasmall Au Nanoparticles Embedded in 2D Mixed-Ligand Metal–Organic Framework Nanosheets Exhibiting Highly Efficient and Size-Selective Catalysis, *Adv. Funct. Mater.*, 2018, **28**(34), 1802021.

133 N. A. Zakaria, R. R. Nasaruddin and W. M. F. Wan Nawawi, Evaluating the potential of chitin extracted from shrimp shell wastes as support material of gold nanoclusters (AuNCs) for catalysis, *IOP Conf. Ser.: Mater. Sci. Eng.*, 2021, **1192**(1), 012032.

134 O. Ramirez, S. Bonardd, C. Saldías, D. Radic and Á. Leiva, Biobased Chitosan Nanocomposite Films Containing Gold Nanoparticles: Obtainment, Characterization, and Catalytic Activity Assessment, *ACS Appl. Mater. Interfaces*, 2017, **9**(19), 16561–16570.

135 P. Abrica-González, J. A. Zamora-Justo, A. Sotelo-López, G. R. Vázquez-Martínez, J. A. Balderas-López and A. Muñoz-Diosdado, *et al.*, Gold nanoparticles with chitosan, N-acylated chitosan, and chitosan oligosaccharide as DNA carriers, *Nanoscale Res. Lett.*, 2019, **14**(1), 258.

136 *Handbook of X-ray photoelectron spectroscopy: a reference book of standard spectra for identification and interpretation of XPS data. Update*, ed. J. F. Moulder and J. Chastain, Perkin-Elmer Corporation, Eden Prairie, Minn, 1992, p. 261.

137 N. Bumbudsanpharoke, J. Choi, I. Park and S. Ko, Facile Biosynthesis and Antioxidant Property of Nanogold-Cellulose Fiber Composite, *J. Nanomater.*, 2015, **2015**, 1–9.

138 D. Berillo, Gold nanoparticles incorporated into cryogel walls for efficient nitrophenol conversion, *J. Cleaner Prod.*, 2020, **247**, 119089.

139 S. Noël, H. Bricout, A. Addad, C. Sonnendecker, W. Zimmermann, E. Monflier and B. Léger, Catalytic reduction of 4-nitrophenol with gold nanoparticles stabilized by large-ring cyclodextrins, *New J. Chem.*, 2020, **44**, 21007–21011.

140 A. Y. Klyushin, T. C. R. Rocha, M. Hävecker, A. Knop-Gericke and R. Schlögl, A near ambient pressure XPS study of Au oxidation, *Phys. Chem. Chem. Phys.*, 2014, **16**(17), 7881.

141 A. Villa, N. Dimitratos, C. E. Chan-Thaw, C. Hammond, G. M. Veith and D. Wang, *et al.*, Characterisation of gold catalysts, *Chem. Soc. Rev.*, 2016, **45**(18), 4953–4994.

142 B. M. Ocko, G. M. Watson and J. Wang, Structure and electrocompression of electrodeposited iodine monolayers on gold (111), *J. Phys. Chem.*, 1994, **98**(3), 897–906.

143 S. A. Wasileski and M. J. Weaver, Electrode Potential-Dependent Anion Chemisorption and Surface Bond Polarization As Assessed by Density Functional Theory, *J. Phys. Chem. B*, 2002, **106**(18), 4782–4788.

144 S. Singh, R. Pasricha, U. M. Bhatta, P. V. Satyam, M. Sastry and B. L. V. Prasad, Effect of halogen addition to monolayer protected gold nanoparticles, *J. Mater. Chem.*, 2007, **17**(16), 1614.

145 Y. Liu, L. Liu and R. Guo, Br^--Induced Facile Fabrication of Spongelike Gold/Amino Acid Nanocomposites and Their Applications in Surface-Enhanced Raman Scattering, *Langmuir*, 2010, **26**(16), 13479–13485.

146 S. H. Kim, E. M. Kim, C. M. Lee, D. W. Kim, S. T. Lim and M. H. Sohn, *et al.*, Synthesis of PEG-Iodine-Capped Gold Nanoparticles and Their Contrast Enhancement in *In Vitro* and *In Vivo* for X-Ray/CT, *J. Nanomater.*, 2012, **2012**(1), 504026.

147 R. Zhou, X. Huang, Q. An, W. Xu, Y. Liu and D. Xu, *et al.*, A Convenient and Sensitive Colorimetric Iodide Assay Based on Directly Inducing Morphological Transformation of Gold Nanostars, *J. Food Drug Anal.*, 2021, **29**(1), 144–152.

148 Y. Xianyu, Y. Lin, Q. Chen, A. Belessiotis-Richards, M. M. Stevens and M. R. Thomas, Iodide-Mediated Rapid and Sensitive Surface Etching of Gold Nanostars for Biosensing, *Angew. Chem., Int. Ed.*, 2021, **60**(18), 9891–9896.
149 W. Cheng, S. Dong and E. Wang, Iodine-Induced Gold-Nanoparticle Fusion/Fragmentation/Aggregation and Iodine-Linked Nanostructured Assemblies on a Glass Substrate, *Angew. Chem., Int. Ed.*, 2003, **42**(4), 449–452.
150 M. Wuithschick, A. Birnbaum, S. Witte, M. Sztucki, U. Vainio and N. Pinna, *et al.*, Turkevich in New Robes: Key Questions Answered for the Most Common Gold Nanoparticle Synthesis, *ACS Nano*, 2015, **9**(7), 7052–7071.
151 E. Agunloye, L. Panariello, A. Gavriilidis and L. Mazzei, A model for the formation of gold nanoparticles in the citrate synthesis method, *Chem. Eng. Sci.*, 2018, **191**, 318–331.
152 X. Ji, X. Song, J. Li, Y. Bai, W. Yang and X. Peng, Size Control of Gold Nanocrystals in Citrate Reduction: The Third Role of Citrate, *J. Am. Chem. Soc.*, 2007, **129**(45), 13939–13948.
153 F. Schulz, T. Homolka, N. G. Bastús, V. Puntes, H. Weller and T. Vossmeyer, Little Adjustments Significantly Improve the Turkevich Synthesis of Gold Nanoparticles, *Langmuir*, 2014, **30**(35), 10779–10784.
154 I. Ojea-Jiménez, N. G. Bastús and V. Puntes, Influence of the Sequence of the Reagents Addition in the Citrate-Mediated Synthesis of Gold Nanoparticles, *J. Phys. Chem. C*, 2011, **115**(32), 15752–15757.
155 S. K. Sivaraman, S. Kumar and V. Santhanam, Monodisperse sub-10nm gold nanoparticles by reversing the order of addition in Turkevich method – The role of chloroauric acid, *J. Colloid Interface Sci.*, 2011, **361**(2), 543–547.
156 S. Monti, G. Barcaro, L. Sementa, V. Carravetta and H. Ågren, Characterization of the adsorption dynamics of trisodium citrate on gold in water solution, *RSC Adv.*, 2017, **7**(78), 49655–49663.
157 D. B. Grys, B. De Nijs, A. R. Salmon, J. Huang, W. Wang and W. H. Chen, *et al.*, Citrate Coordination and Bridging of Gold Nanoparticles: The Role of Gold Adatoms in AuNP Aging, *ACS Nano*, 2020, **14**(7), 8689–8696.
158 J. W. Park and J. S. Shumaker-Parry, Structural Study of Citrate Layers on Gold Nanoparticles: Role of Intermolecular Interactions in Stabilizing Nanoparticles, *J. Am. Chem. Soc.*, 2014, **136**(5), 1907–1921.
159 R. Ciganda, N. Li, C. Deraedt, S. Gatard, P. Zhao and L. Salmon, *et al.*, Gold nanoparticles as electron reservoir redox catalysts for 4-nitrophenol reduction: a strong stereoelectronic ligand influence, *Chem. Commun.*, 2014, **50**(70), 10126–10129.
160 B. M. Quinn, P. Liljeroth, V. Ruiz, T. Laaksonen and K. Kontturi, Electrochemical Resolution of 15 Oxidation States for Monolayer Protected Gold Nanoparticles, *J. Am. Chem. Soc.*, 2003, **125**(22), 6644–6645.
161 S. Chen and K. Huang, Electrochemical and Spectroscopic Studies of Nitrophenyl Moieties Immobilized on Gold Nanoparticles, *Langmuir*, 2000, **16**(4), 2014–2018.
162 Y. Zhang, S. Liu, H. Xie, X. Zeng and J. Li, Current Status on Leaching Precious Metals from Waste Printed Circuit Boards, *Procedia Environ. Sci.*, 2012, **16**, 560–568.
163 A. Tuncuk, V. Stazi, A. Akcil, E. Y. Yazici and H. Deveci, Aqueous metal recovery techniques from e-scrap: Hydrometallurgy in recycling, *Miner. Eng.*, 2012, **25**(1), 28–37.
164 L. Zhang and Z. Xu, A review of current progress of recycling technologies for metals from waste electrical and electronic equipment, *J. Cleaner Prod.*, 2016, **127**, 19–36.
165 C. J. Oh, S. O. Lee, H. S. Yang, T. J. Ha and M. J. Kim, Selective Leaching of Valuable Metals from Waste Printed Circuit Boards, *J. Air Waste Manage. Assoc.*, 2003, **53**(7), 897–902.
166 P. Cyganowski, K. Garbera, A. Leśniewicz, J. Wolska, P. Pohl and D. Jermakowicz-Bartkowiak, The recovery of gold from the aqua regia leachate of electronic parts using a core–shell type anion exchange resin, *J. Saudi Chem. Soc.*, 2017, **21**(6), 741–750.
167 M. Mann, T. Nicholls, H. Patel, L. Lisboa, J. Pople and L. N. Pham, *et al.*, Integrated methods for gold leaching and recovery from ore and electronic waste, *Chemistry*, 2024, **1**, 1–18.
168 H. Niu, H. Yang and L. Tong, Gold recovery from chloride leach solution of TCCA using D301 anion exchange resin and elution with thiourea, *Hydrometallurgy*, 2024, **230**(106384), 1–12.
169 J. M. Chalker, Materials and processes for recovering precious metals, US20220205061A1, 2022.
170 U. Tilstam and H. Weinmann, Trichloroisocyanuric Acid: A Safe and Efficient Oxidant, *Org. Process Res. Dev.*, 2002, **6**(4), 384–393.
171 S. Gaspa, M. Carraro, L. Pisano, A. Porcheddu and L. De Luca, Trichloroisocyanuric Acid: a Versatile and Efficient Chlorinating and Oxidizing Reagent, *Eur. J. Org. Chem.*, 2019, **2019**(22), 3544–3552.
172 G. Mendonca and M. Mattos, Green Chlorination of Organic Compounds Using Trichloroisocyanuric Acid (TCCA), *Curr. Org. Synth.*, 2014, **10**(6), 820–836.
173 F. Anjum, S. Gul, M. Khan and M. A. Khan, Efficient synthesis of palladium nanoparticles using gugar gum as stabiliser and their applications as catalyst in reduction reactions and degradation of azo dyes, *Green Process. Synth.*, 2020, **9**, 63–76.
174 M. T. Islam, R. Saena-Arana, H. Wang, R. Bernal and J. C. Noveron, Green synthesis of gold, silver, platinum, and palladium nanoparticles reduced and stabilized by sodium rhodizonate and their catalytic reduction of 4-nitrophenol and methyl orange, *New J. Chem.*, 2018, **42**(8), 6472–6478.
175 Y. R. Mejía and N. K. Reddy Bogireddy, Reduction of 4-nitrophenol using green-fabricated metal nanoparticles, *RSC Adv.*, 2022, **12**(29), 18661–18675.
176 H. Veisi, B. Karmakar, T. Tamoradi, R. Tayebee, S. Sajjadifar and S. Lotfi, *et al.*, Bio-inspired synthesis of palladium nanoparticles fabricated magnetic Fe3O4 nanocomposite

over Fritillaria imperialis flower extract as an efficient recyclable catalyst for the reduction of nitroarenes, *Sci. Rep.*, 2021, **11**(1), 4515.

177 L. S. Johansson, J. M. Campbell, K. Koljonen and P. Stenius, Evaluation of surface lignin on cellulose fibers with XPS, *Appl. Surf. Sci.*, 1999, **144–145**, 92–95.

178 Y. Bourlier, M. Bouttemy, O. Patard, P. Gamarra, S. Piotrowicz and J. Vigneron, *et al.*, Investigation of InAlN Layers Surface Reactivity after Thermal Annealings: A Complete XPS Study for HEMT, *ECS J. Solid State Sci. Technol.*, 2018, **7**(6), P329–P338.

179 B. Zhang, T. Zhang, Y. Duan, Z. Zhao, X. Huang and X. Bai, *et al.*, Human exposure to phthalate esters associated with e-waste dismantling: Exposure levels, sources, and risk assessment, *Environ. Int.*, 2019, **124**, 1–9.

180 K. Li and Z. Xu, Decomposition of high-impact polystyrene resin in e-waste by supercritical water oxidation process with debromination of decabromodiphenyl ethane and recovery of antimony trioxide simultaneously, *J. Hazard. Mater.*, 2021, **402**, 123684.

181 A. Ahrens, A. Bonde, H. Sun, N. K. Wittig, H. C. D. Hammershøj and G. M. F. Batista, *et al.*, Catalytic disconnection of C–O bonds in epoxy resins and composites, *Nature*, 2023, **617**(7962), 730–737.

182 C. Fromonteil, P. Bardelle and F. Cansell, Hydrolysis and Oxidation of an Epoxy Resin in Sub- and Supercritical Water, *Ind. Eng. Chem. Res.*, 2000, **39**(4), 922–925.

183 J. Delozanne, N. Desgardin, N. Cuvillier and E. Richaud, Thermal oxidation of aromatic epoxy-diamine networks, *Polym. Degrad. Stab.*, 2019, **166**, 174–187.

184 V. A. Kumar, T. Uchida, T. Mizuki, Y. Nakajima, Y. Katsube and T. Hanajiri, *et al.*, Synthesis of nanoparticles composed of silver and silver chloride for a plasmonic photocatalyst using an extract from a weed *Solidago altissima* (goldenrod), *Adv. Nat. Sci.: Nanosci. Nanotechnol.*, 2016, **7**(1), 015002.

185 C. A. Strydom, J. F. Van Staden and H. J. Strydom, An XPS investigation of silver chloride coated ion-selective electrodes, *J. Electroanal. Chem. Interfacial Electrochem.*, 1990, **277**(1–2), 165–177.

186 N. Toyama, H. Kimura, N. Matsumoto, S. Kamei, D. N. Futaba and N. Terui, *et al.*, Enhanced activity for reduction of 4-nitrophenol of Ni/single-walled carbon nanotube prepared by super-growth method, *Nanotechnology*, 2022, **33**(6), 065707.

187 P. Boonying, S. Martwiset and S. Amnuaypanich, Highly catalytic activity of nickel nanoparticles generated in poly(methylmethacrylate)@poly(2-hydroxyethylmethacrylate) (PMMA@PHEMA) core–shell micelles for the reduction of 4-nitrophenol (4-NP), *Appl. Nanosci.*, 2018, **8**(3), 475–488.

188 A. Lourens, A. Falch and R. Malgas-Enus, Nano-Ni/Cu decorated iron oxide for catalytic reduction of 4-nitrophenol, *Mater. Chem. Phys.*, 2024, **315**, 129022.

189 W. Xia, F. Zhao, P. Fang, M. An, J. Zhu and K. Cheng, *et al.*, Magnetic Fe3O4@C nanoparticles separated from cold rolling mill sludge for 4-nitrophenol reduction, *Sep. Purif. Technol.*, 2023, **309**, 123018.

190 R. Widmer, H. Oswald-Krapf, D. Sinha-Khetriwal, M. Schnellmann and H. Böni, Global perspectives on e-waste, *Environ. Impact Assess. Rev.*, 2005, **25**(5), 436–458.

191 M. Beck, *Recycling Magazine Benelux*, Recycling International, 2008, vol. 2.

192 N. Wong, Electronic Waste Governance under "One Country, Two Systems": Hong Kong and Mainland China, *Int. J. Environ. Res. Public Health*, 2018, **15**(11), 2347.